

Accepted Manuscript

Alkynyl-containing phenylthiazoles: Systemically active antibacterial agents effective against methicillin-resistant *Staphylococcus aureus* (MRSA)

Mohamed M. Elsebaei, Haroon Mohammad, Mohamed Abouf, Nader S. Abutaleb, Youssef A. Hegazy, Adel Ghiaty, Lu Chen, Jianan Zhang, Satish R. Malwal, Eric Oldfield, Mohamed N. Seleem, Abdelrahman S. Mayhoub

PII: S0223-5234(18)30161-2

DOI: [10.1016/j.ejmech.2018.02.031](https://doi.org/10.1016/j.ejmech.2018.02.031)

Reference: EJMECH 10208

To appear in: *European Journal of Medicinal Chemistry*

Received Date: 4 January 2018

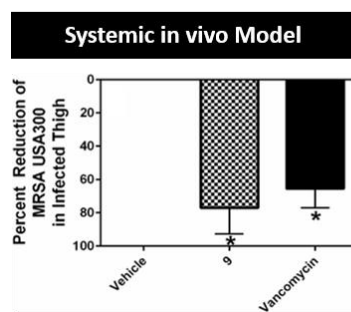
Revised Date: 9 February 2018

Accepted Date: 10 February 2018

Please cite this article as: M.M. Elsebaei, H. Mohammad, M. Abouf, N.S. Abutaleb, Y.A. Hegazy, A. Ghiaty, L. Chen, J. Zhang, S.R. Malwal, E. Oldfield, M.N. Seleem, A.S. Mayhoub, Alkynyl-containing phenylthiazoles: Systemically active antibacterial agents effective against methicillin-resistant *Staphylococcus aureus* (MRSA), *European Journal of Medicinal Chemistry* (2018), doi: 10.1016/j.ejmech.2018.02.031.

This is a PDF file of an unedited manuscript that has been accepted for publication. As a service to our customers we are providing this early version of the manuscript. The manuscript will undergo copyediting, typesetting, and review of the resulting proof before it is published in its final form. Please note that during the production process errors may be discovered which could affect the content, and all legal disclaimers that apply to the journal pertain.

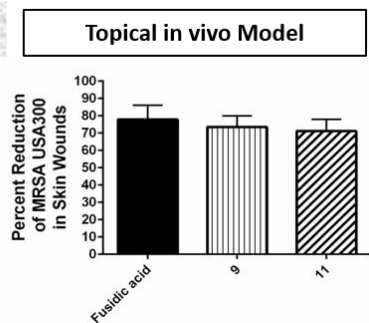
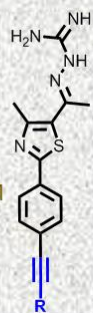




Bacteriological profile:
 MIC (MRSA)= 0.5-2 $\mu\text{g}/\text{mL}$
 MIC (VRSA)= 0.5-2 $\mu\text{g}/\text{mL}$
 Fast bactericidal agents
 Active against intracellular MRSA

Biochemical assays:
 IC_{50} (UPPP)= 6 μM ; IC_{50} (UPPS)= 19 μM

In vivo PK profile:
 $t_{1/2}$ > 4.4 h; CL= 5.6 L/hr; Vd= 18.5 L
 Stable to hepatic metabolism



ACCEPTED MANUSCRIPT

**Alkynyl-Containing Phenylthiazoles: Systemically Active Antibacterial Agents Effective
Against Methicillin-resistant *Staphylococcus aureus* (MRSA)**

Mohamed M. Elsebaei,^{a,†} Haroon Mohammad,^{b,†} Mohamed Abouf,^a Nader S. Abutaleb,^b Youssef

A. Hegazy,^b Adel Ghiaty,^a Lu Chen,^c Jianan Zhang,^d Satish R. Malwal,^f Eric Oldfield,^{e,f}

Mohamed N. Seleem,^{b,g,**} and Abdelrahman S. Mayhoub^{a,h*}

^{a.} Department of Pharmaceutical Organic Chemistry, College of Pharmacy, Al-Azhar University, Cairo 11884, Egypt.

^{b.} Department of Comparative Pathobiology, Purdue University, College of Veterinary Medicine, West Lafayette, IN 47907, USA.

^{c.} Department of Biochemistry, University of Illinois at Urbana-Champaign, Urbana, IL, 61801, United States

^{d.} School of Molecular and Cellular Biology, University of Illinois at Urbana-Champaign, Urbana, IL, 61801, United States

^{e.} Center for Biophysics and Quantitative Biology, University of Illinois at Urbana-Champaign, Urbana, IL, 61801, United States

^{f.} Department of Chemistry, University of Illinois at Urbana-Champaign, Urbana, IL, 61801, United States

^{g.} Purdue Institute for Inflammation, Immunology, and Infectious Diseases, West Lafayette, IN 479067, USA.

^{h.} University of Science and Technology, Zewail City of Science and Technology, Giza, Egypt

[†]: These authors contributed equally to this work

Corresponding Authors

** MNS; email, mseleem@purdue.edu

* ASM; e-mail, amayhoub@azhar.edu.eg

Abbreviations. Caco-2, heterogeneous human epithelial colorectal adenocarcinoma cells; CFUs, colony forming units; HaCaT, human keratinocytes; P_{app} , apparent permeability; VISA, vancomycin-intermediate *S. aureus*; HBD, hydrogen bond donor; P-gp, P-glycoprotein.

Key words. Antibiotic resistance, MRSA, VRSA, multi-drug resistance, *C. elegans*

1. ABSTRACT

The promising activity of phenylthiazoles against multidrug-resistant bacterial pathogens, in particular MRSA, has been hampered by their limited systemic applicability, due to their rapid metabolism by hepatic microsomal enzymes, resulting in short half-lives. Here, we investigated a series of phenylthiazoles with alkynyl side-chains that were synthesized with the objective of improving stability to hepatic metabolism, extending the utility of phenylthiazoles from topical applications to treatment of a more invasive, systemic MRSA infections. The most promising compounds inhibited the growth of clinically-relevant isolates of MRSA *in vitro* at concentrations as low as 0.5 $\mu\text{g/mL}$, and exerted their antibacterial effect by interfering with bacterial cell wall synthesis *via* inhibition of undecaprenyl diphosphate synthase and undecaprenyl diphosphate phosphatase. We also identified two phenylthiazoles that successfully eradicated MRSA inside infected macrophages. *In vivo* PK analysis of compound **9** revealed promising stability to hepatic metabolism with a biological half-life of ~ 4.5 hours. In mice, compound **9** demonstrated comparable potency to vancomycin, and at a lower dose (20 mg/kg *versus* 50 mg/kg), in reducing the burden of MRSA in a systemic, deep-tissue infection, using the neutropenic mouse thigh-infection model. Compound **9** thus represents a new phenylthiazole lead for the treatment of MRSA infections that warrants further development.

2. INTRODUCTION

In recent years, the number of fatal infections caused by antibiotic-resistant bacteria has increased in many regions around the world. *Staphylococcus aureus* is a prominent bacterial pathogen responsible for a diverse array of infections ranging from superficial skin lesions to invasive diseases including soft-tissue infections, pneumonia, endocarditis, and osteomyelitis. The emergence in the 1960s of *S. aureus* isolates exhibiting resistance to β -lactam antibiotics such as methicillin, methicillin-resistant *S. aureus* or MRSA, spurred several outbreaks in hospitals [1]. Treatment of MRSA infections for clinicians has become exacerbated by the emergence of strains exhibiting resistance to other antibiotic classes, including fluoroquinolones, tetracyclines, macrolides, lincosamides and aminoglycosides [2]. More recently, strains of drug-resistant *S. aureus* have emerged that exhibit intermediate sensitivity or resistance to vancomycin (VISA and VRSA, respectively), an antibiotic that has been the cornerstone treatment choice for MRSA infections [3]. Though several antibiotics are currently in the clinical pipeline, the vast majority of these agents are derivatives of existing antibiotic classes that do not exert their effects by attacking new molecular targets. Thus, developing new antibacterial agents with unique chemical scaffolds and molecular target(s), effective against MRSA, still remains a critical issue for the medicinal chemistry community to address [4].

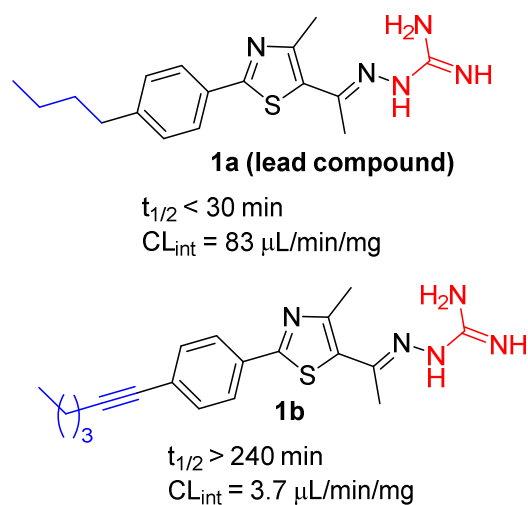


Figure 1. Chemical structures of two first-generation phenylthiazole lead compounds with their half-life ($t_{1/2}$) and intrinsic clearance (CL_{int}) values identified using human liver microsomes.

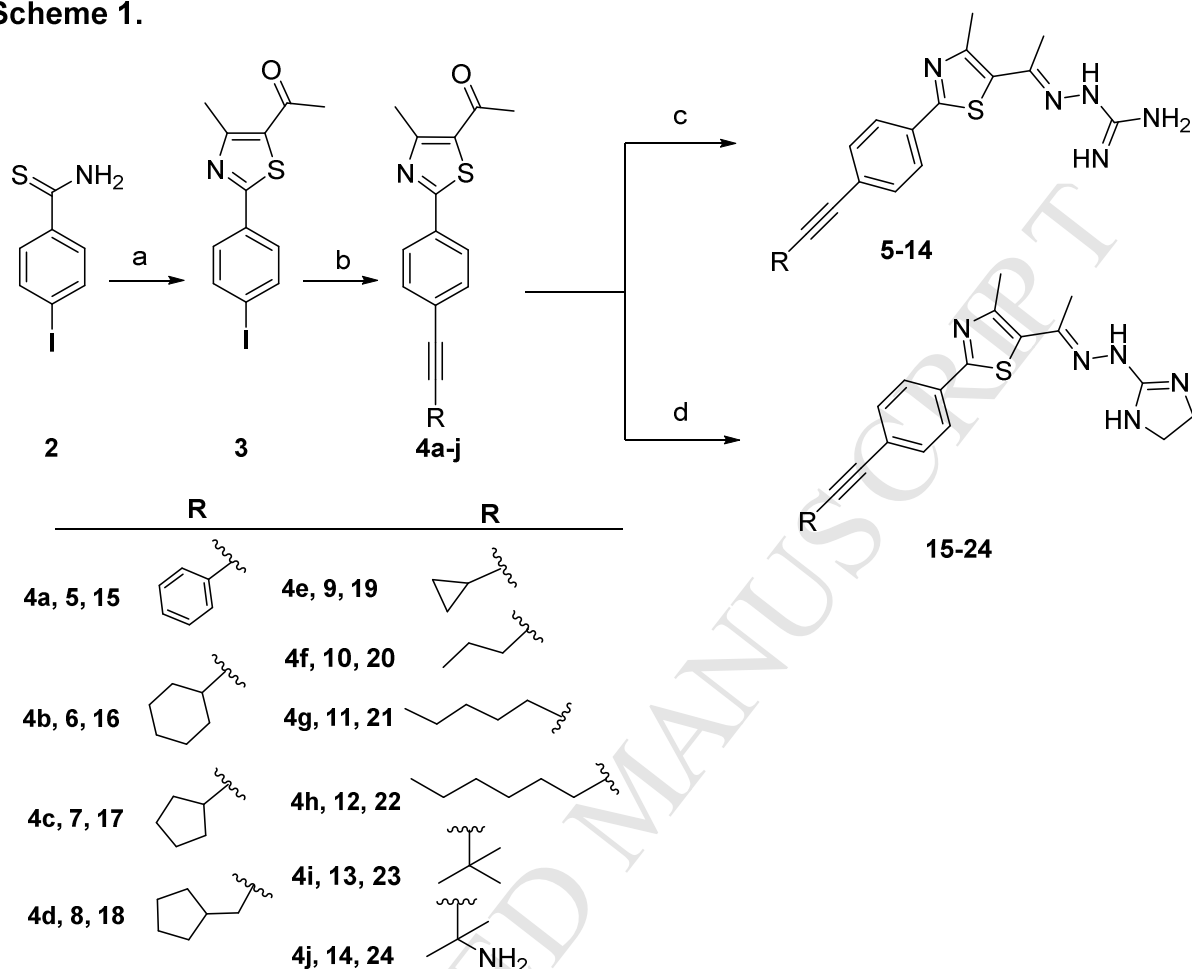
Recognizing the need for new antibacterial agents, we have been investigating compounds containing the phenylthiazole scaffold for the development of antibacterial agents [5]. The first-generation phenylthiazoles we synthesized exhibited antibacterial activity against key Gram-positive pathogens, including MRSA and vancomycin-resistant enterococci, by interfering with bacterial cell wall synthesis [6]. However, the compounds were susceptible to rapid metabolism ($t_{1/2} < 30$ minutes), with the exception of the hexynyl derivative **1b** ($t_{1/2} > 4$ hours), which was not effective *in vivo* in treating a MRSA infection (Figure 1) [5c]. Incorporating the imine bond of the lead compound **1a** within a pyrimidine ring yielded second-generation phenylthiazoles with enhanced stability to hepatic metabolism [5d], and a complete metabolite analysis of **1a** indicated the presence of an additional metabolic "soft spot" at the butyl benzylic carbon [7]. Removing this soft spot has the potential to yield phenylthiazole compounds with better stability to hepatic metabolism. To address this, the *n*-butyl group of the lead compound **1a** was replaced with an array of alkynyl side-chains having different sizes and

spatial configurations. The antibacterial activity of the new analogues was then examined against a broad panel of drug-resistant *S. aureus* clinical isolates, and the metabolic stability and permeability profiles of the most promising analogues assessed. Additionally, the ability of the most promising analogue (compound **9**) to inhibit the molecular targets of the first-generation phenylthiazoles (undecaprenyl diphosphate synthase, UPPS, and undecaprenyl diphosphate phosphatase, UPPP) was investigated. Furthermore, compound **9** was evaluated in three different animal models of MRSA infection: *Caenorhabditis elegans*; an uncomplicated skin infection mouse model, and a neutropenic thigh-infection mouse model.

3. RESULTS AND DISCUSSION

3.1. Chemistry. The key starting compound **3** was prepared as reported [5a], by treatment of *p*-iodothioamide (**2**) with α -chloroacetylacetone. The corresponding *p*-alkynyl analogues **4a-j** were obtained using standard Sonogashira carbon-carbon cross-coupling conditions (Scheme 1). Condensation of **4a-j** with aminoguanidine hydrochloride or 2-hydrazino-2-imidazoline hydrobromide yielded the final products **5-24** (Scheme 1).

Scheme 1.



Reagents and conditions: (a) Absolute EtOH, 3-chloropentane-2,4-dione, heat to reflux, 12 h; (b) PdCl₂(PPh₃)₂ (5% mol), CuI (7.5% mol), CsCO₃, Et₃N, DMF, heat at 50°C for 24 h; (c) aminoguanidine HCl, EtOH, Conc. HCl, heat to reflux 4 h; (d) 2-hydrazino-2-imidazoline HBr, EtOH, conc. HCl, heat to reflux 4 h.

3.2. Antibacterial Activity of New Compounds Against MRSA. Initially, the antibacterial activity of the new analogues was examined against MRSA USA300, a strain responsible for the majority of *S. aureus* skin and soft-tissue infections (SSTIs) [8], community-acquired MRSA (CA-MRSA) infections [8], and MRSA-induced pneumonia [9]. The phenylethynyl derivative **5** inhibited MRSA USA300 at a concentration of 1 µg/mL (Table 1), similar to vancomycin (Table 1). Replacement of the terminal phenyl ring with alicyclic moieties generated compounds **6**, **7**

and **9** with cyclohexyl (**6**), cyclopentyl (**7**) and cyclopropyl (**9**) rings. These three alicyclic-containing derivatives inhibited MRSA growth at 2 $\mu\text{g/mL}$ (Table 1). Separating the terminal alicyclic ring from the ethynyl moiety via a methylene unit provided compound **8**. This derivative was less active against MRSA USA300 (minimum inhibitory concentration (MIC) value of **8** = 4 $\mu\text{g/mL}$, Table 1). The linear analogues, **10-12**, inhibited MRSA at concentrations ranging from 1 to 4 $\mu\text{g/mL}$ (Table 1). Similarly, the antibacterial activity of the branched analogue **13** was on par with the linear derivatives **11** and **12** (Table 1). Insertion of a polar group within the lipophilic region (compound **14**) abolished the compound's anti-MRSA activity (Table 1).

As we have reported before, the guanidinyll head is an essential structural element for tphenylthiazole anti-MRSA activity [5a]; however, it is also responsible for high affinity to the P-gp efflux system [5a]. A strategy to decrease P-gp affinity is to decrease the number of HBD's [10]. Therefore, hydrazino-2-imidazolinyll analogues **15-24** were synthesized, with only two HBD's, and their anti-MRSA activity was initially evaluated against MRSA USA300 (Table 1). In general, all imidazolinyll analogues were at least one-fold less potent than the corresponding guanidinyll analogues (Table 1).

Table 1. The minimum inhibitory concentration (MIC in $\mu\text{g/mL}$) and the minimum bactericidal concentration (MBC $\mu\text{g/mL}$) of compounds and vancomycin screened against MRSA USA300.

Compound	MIC	MBC
5	1	1
6	2	4
7	2	4
8	4	4
9	2	4
10	1	8
11	4	4
12	4	8
13	4	4
14	64	64

15	8	16
16	8	8
17	4	16
18	8	32
19	8	16
20	>64	>64
21	4	8
22	8	16
23	2	4
24	>64	>64

Next, the antibacterial **Vancomycin** activity of twelve derivatives exhibiting the most potent activity against MRSA USA300 was evaluated against six additional clinical isolates of drug-resistant *S. aureus*, including three vancomycin-resistant isolates (Table 2). The compounds inhibited growth of clinical isolates (MICs ranged from 0.5 to 4 $\mu\text{g/mL}$) of *S. aureus* exhibiting high-level resistance to the antibiotics mupirocin (NRS107) and linezolid (NRS119). Additionally, all compounds were significantly more potent ($> 100\times$) than vancomycin against clinical isolates of vancomycin-resistant *S. aureus* (VRS10, VRS11a, and VRS12) (Table 2). For example, the pentynyl derivative **10** inhibited growth of VRS11a at a concentration of 0.5 $\mu\text{g/mL}$. In contrast, the MIC of vancomycin against VRS11a exceeded 512 $\mu\text{g/mL}$.

Table 2. Minimum inhibitory concentration (MIC in $\mu\text{g/mL}$) and minimum bactericidal concentration (MBC $\mu\text{g/mL}$) of active compounds screened against additional *S. aureus* isolates.

Compound Name	<i>S. aureus</i> NRS107		MRSA NRS119		MRSA NRS123 (USA400)		VRS10 (VRSA)		VRS11a (VRSA)		VRS12 (VRSA)	
	MIC	MBC	MIC	MBC	MIC	MBC	MIC	MBC	MIC	MBC	MIC	MBC
5	2	2	1	2	1	4	1	2	1	2	2	2
6	16	16	4	4	2	2	2	2	1	2	2	2
7	2	2	1	2	2	2	2	2	1	4	2	2
8	2	4	4	4	2	2	2	4	4	4	2	2
9	2	2	2	2	2	2	2	4	2	2	2	2
10	1	1	1	1	≤ 0.5	2	1	2	≤ 0.5	≤ 0.5	1	1

Compound Name	<i>S. aureus</i> NRS107		MRSA NRS119		MRSA NRS123 (USA400)		VRS10 (VRSA)		VRS11a (VRSA)		VRS12 (VRSA)	
	MIC	MBC	MIC	MBC	MIC	MBC	MIC	MBC	MIC	MBC	MIC	MBC
11	2	4	2	2	2	2	2	2	1	2	2	2
12	4	8	1	4	4	4	2	4	0.5	2	2	4
13	2	4	2	2	4	16	4	4	2	8	4	4
17	16	32	32	32	16	32	4	8	8	8	16	16
21	16	32	16	32	16	32	8	64	8	16	16	32
23	2	4	2	2	4	16	4	4	4	4	4	8
Vancomycin	1	1	1	1	1	1	512	512	>512	>512	16	256

In agreement with the first- and second-generation phenylthiazoles, the new analogues possessed minimum bactericidal concentration (MBC) values that were either identical to or up to three-fold higher than their MIC values against MRSA and VRSA (Tables 1 and 2). This observation indicates the new phenylthiazoles are bactericidal. To confirm this, six compounds (**5**, **6**, **7**, **9**, **10**, and **11** all at $4 \times \text{MIC}$) were analyzed against MRSA via a time-kill assay.

As shown in Figure 2A, phenylthiazoles containing linear side chains (**10** and **11**) exhibited rapid bactericidal activity against MRSA (complete eradication observed after 2 and 4 hours, respectively). On the other hand, the cyclohexyl-containing compound **6** gradually reduced MRSA CFU/mL from 1.9-log_{10} (after 4 hours) to 2.8-log_{10} (after 12 hours) and eventually generated a 4.3-log_{10} reduction in CFU/mL after 24 hours. The two alicyclic-containing compounds **7** and **9** behaved differently (Figure 2B). Compound **7** generated a near 3-log_{10} reduction in MRSA CFU/mL after 8 hours, but bacterial re-growth was observed thereafter. Compound **9** exhibited slow bactericidal activity against MRSA, similar to vancomycin [10]. Both agents gradually reduced MRSA CFU/mL resulting in complete eradication of MRSA USA400 after 24 hours. The rapid bactericidal characteristic observed with compounds **10** and

11 *in vitro* against MRSA may be beneficial in helping to clear an infection *in vivo*, particularly for invasive infections such as endocarditis [10]. From a SAR perspective: there is a strong correlation between antibacterial kinetics and the size and spatial configuration of the lipophilic side chain. Compound **5**, consisting of the phenylethynyl tail, is bacteriostatic. Removal of the aromaticity of the terminal phenyl ring (compound **6**) improved, bactericidal activity—the rate of bacterial clearance. Furthermore, decreasing the size of the terminal ring by substituting the cyclohexyl group of compound **6** with the cyclopropyl group in compound **9**, yielded a compound with slow bactericidal activity. Finally, replacement of the terminal phenyl ring of **5** with a linear alkyne chain (compounds **10** and **11**) changed the bacteriostatic effect observed, to rapid bactericidal action against MRSA.

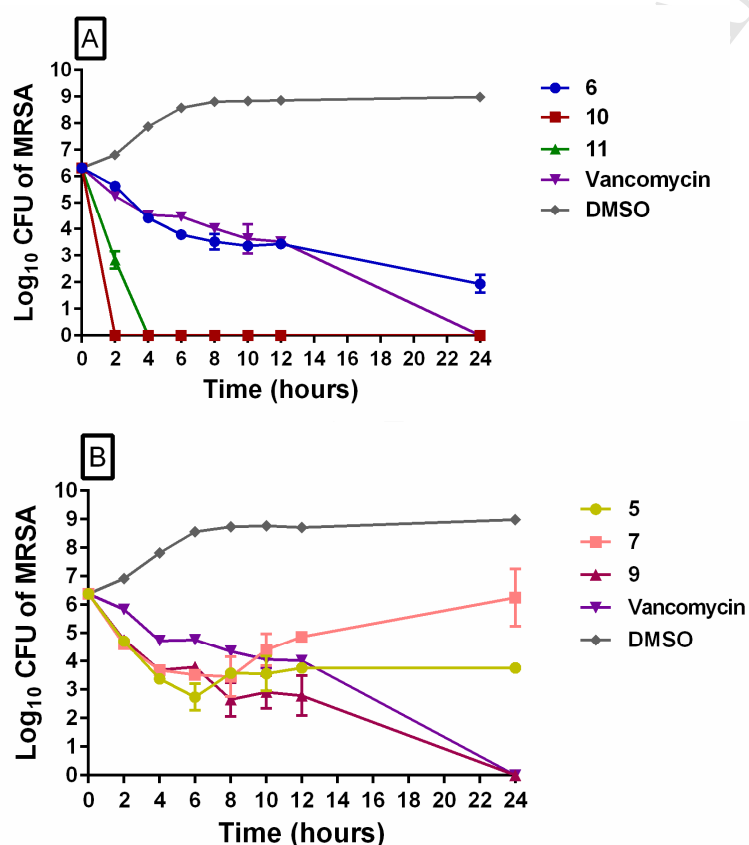


Figure 2: Time-kill analysis of compounds against MRSA A) compounds **6**, **10** and **11**, and vancomycin and B) compounds **5**, **7** and **9**, and vancomycin against MRSA over a 24-hour

incubation period at 37 °C. DMSO served as a negative control. The error bars represent standard deviation values obtained from triplicate samples used for each compound/antibiotic studied.

3.3. Investigating the Ability of the Phenylthiazole Analogues to Clear an Intracellular

MRSA Infection. Given the alkynylphenylthiazole bactericidal activity against extracellular MRSA, we next moved to evaluate activity against intracellular MRSA. MRSA utilizes multiple approaches to evade the host's immune response to clearing an infection. One mechanism involves MRSA invading, and surviving, inside host immune cells—including macrophages [13]. This tactic leads to recurring infections that are recalcitrant to antibiotic treatment [14], because the antibiotics that are frequently used to treat MRSA infections, primarily vancomycin, fail to clear intracellular MRSA. This is due, at least in part, to poor penetration into infected macrophages [15]. In this regard, pneumonia-induced MRSA has resulted in clinical failure in more than 40% of cases treated with the standard vancomycin dosing regimen [16]. We thus next investigated the ability of the alkynylphenylthiazoles to penetrate and target MRSA harboring inside macrophages (J774) (Figure 3).

We first tested compounds for toxicity to macrophage cells. After a 24-hour incubation of compounds with J774 cells, viability was assessed via MTS assay. Compounds **6**, **10**, and **11** were found to be non-toxic to macrophage cells up to a concentration of 16 µg/mL, while compounds **7** and **9** were non-toxic up to 8 µg/mL (Figure 3A,C). Next, compounds (utilizing the highest concentration where no toxicity was observed) were evaluated for their ability to reduce the burden of MRSA inside infected macrophages. Derivatives with linear alkyne side chains, **10** and **11**, resulted in complete eradication of intracellular MRSA. In contrast, neither the alicyclic-containing derivatives **6**, **7** or **9** ($4 \times \text{MIC}$) nor vancomycin ($4 \times \text{MIC}$) were able to produce a significant reduction in the burden of intracellular MRSA, in comparison to the untreated control

(Figure 3B). Interestingly, there appears to be a close association between the results obtained with the time-kill assay and the ability of the compounds to clear MRSA harboring inside macrophages. Compounds **10** and **11** exhibited rapid bactericidal activity in the time-kill assay (completely eradicated a high inoculum of MRSA within four hours), and these two compounds were able to clear intracellular MRSA harboring inside infected macrophages. In contrast, compounds **6**, **9**, and vancomycin exhibited slow bactericidal activity in the time-kill assay (**9** and vancomycin completely reduced MRSA CFU to zero only after 24 hours). The clinical failure rate of standard vancomycin treatment of MRSA-induced pneumonia has been attributed in part to its time-dependent, slow bactericidal activity [15, 17]. Thus, the presence of the linear alkyne side chain in compounds **10** and **11** appears to be beneficial in two aspects: contributing to rapid bactericidal activity against extracellular MRSA, and permitting the compounds to penetrate and clear MRSA harboring inside infected macrophages.

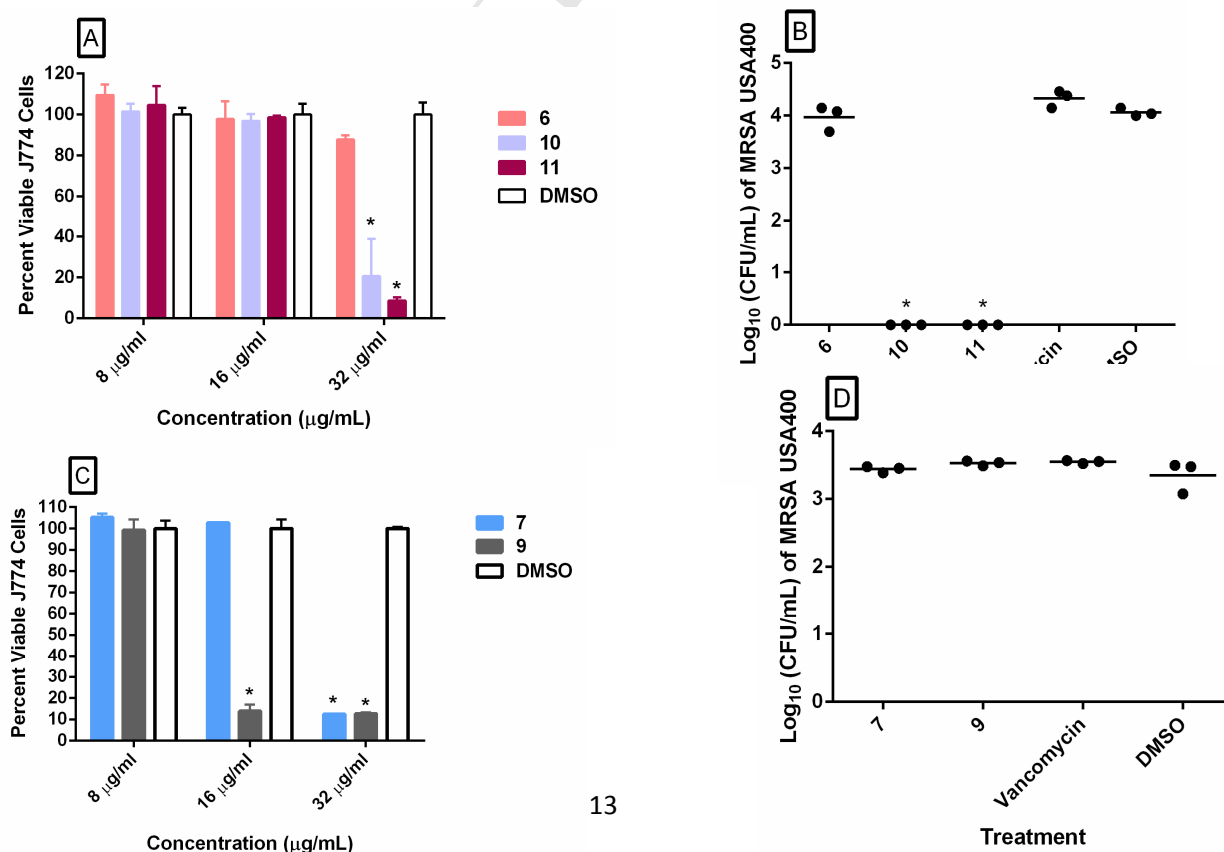


Figure 3. Toxicity analysis and examination of clearance of intracellular MRSA present in murine macrophage (J774) cells.

A) Percent viable mammalian cells (measured as average absorbance ratio (test agent relative to DMSO)) for cytotoxicity analysis of compounds **6**, **10**, and **11** (tested in triplicate) at 8, 16, and 32 $\mu\text{g/mL}$ against J774 cells using the MTS 3-(4,5-dimethylthiazol-2-yl)-5-(3-carboxymethoxyphenyl)-2-(4-sulfophenyl)-2H-tetrazolium) assay. Dimethyl sulfoxide (DMSO) was used as a negative control to determine a baseline measurement for the cytotoxic impact of each compound. The absorbance values represent an average of a minimum of three samples analyzed for each compound. Error bars represent standard deviation values for the absorbance values. A Student t-test with post-hoc Holm-Sidak test, ($P < 0.05$), determined statistical difference between the values obtained for each compound and DMSO (denoted by the asterisk) ($P < 0.05$). **B)** Percent reduction of MRSA USA400 colony forming units inside infected macrophage (J774) cells after treatment with 16 $\mu\text{g/mL}$ of compounds **6**, **10**, and **11**, and with 4 $\mu\text{g/mL}$ vancomycin (tested in triplicate) for 24 hours. Data was analyzed using a Student's t-test. Asterisks (*) indicate statistically significant difference between treatment with compounds **10** and **11** in relation to DMSO-treated wells ($P < 0.05$). **C)** Percent viable mammalian cells (measured as average absorbance ratio (test agent relative to DMSO)) for cytotoxicity analysis of compounds **7** and **9** (tested in triplicate) at 8, 16, and 32 $\mu\text{g/mL}$ against J774 cells using the MTS 3-(4,5-dimethylthiazol-2-yl)-5-(3-carboxymethoxyphenyl)-2-(4-sulfophenyl)-2H-tetrazolium) assay. Error bars represent standard deviation values for the absorbance values. A Student's t-test with post-hoc Holm-Sidak test, ($P < 0.05$), determined statistical difference between the values obtained for each compound and DMSO (denoted by the asterisk) ($P < 0.05$). **D)** Percent reduction of MRSA USA400 colony forming units inside infected macrophage (J774) cells after treatment with 8 $\mu\text{g/mL}$ of compounds **7**, **9**, and vancomycin (tested in triplicate) for 24 hours.

3.4. Toxicity Assessment Using Human Colorectal Cells. After confirming the antibacterial activity of the new phenylthiazole derivatives against drug-resistant *S. aureus*, we next sought to investigate possible cytotoxicity against a human cell line (colorectal cells; HRT-18). Compounds **5**, **6**, **7**, **9**, **10**, **11**, **12**, **13** and **23** were found to be non-toxic up to 32 $\mu\text{g/mL}$ (Figure 4). This represents a 7- to 31-fold difference between the MIC values obtained against MRSA and the concentration where the compounds toxic to these mammalian cells.

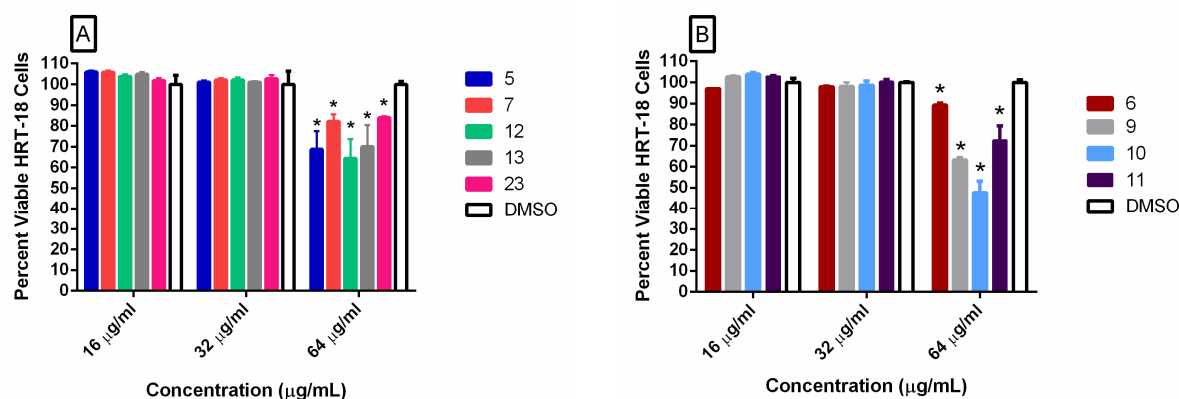


Figure 4: Examination of toxicity of new phenylthiazole analogues against human colorectal cells (HRT-18) A) Toxicity analysis of tested compounds **5**, **7**, **12**, **13**, and **23**. B) Toxicity analysis of compounds **6**, **9**, **10**, and **11**.

3.5. Mechanism of Action of 9. In order to determine whether the new compounds have the same mechanism of antibacterial action to that of the original lead thiazole compound (**1a**), compound **9** was selected for further analysis. In previous work, [6] we found that **1a** was an inhibitor of bacterial cell wall synthesis, inhibiting both undecaprenyl diphosphate phosphatase ($IC_{50} = 6 \mu M$) and undecaprenyl diphosphate synthase ($IC_{50} = 19 \mu M$), in addition to being a weak protonophore uncoupler (in inverted membrane vesicles; $IC_{50} \sim 12-25 \mu M$). To determine to what extent **9** had similar effects, we used the *E. coli* UPPP expression system described previously and determined the IC_{50} for inhibition by **9** [18]. We found an $8.1 \mu M$ IC_{50} (corresponding to $2.7 \mu g/mL$), consistent with a UPPP target, Figure 5A. Under these assay conditions, the antibiotic bacitracin has a $5.6 \mu M$ IC_{50} ($1.9 \mu g/mL$), as reported previously [6], but shown again here for convenience (Figure 5A). We also tested for human FPPS (HsFPPS) and *E. coli* UPPS (EcUPPS) inhibition. There was no inhibition of HsFPPS (data not shown), but UPPS was inhibited with a $38 \mu M$ IC_{50} (corresponding to $13 \mu g/mL$), Figure 5B, weaker than known potent UPPS inhibitors, such as NSC-50460 (Figure 5B). Since UPPS and UPPP are

adjacent to each other in the cell wall biosynthetic pathway, such multi-target inhibition may nevertheless contribute to the activity of **9**, similar to the dual UPPS/UPPP inhibition we have reported with other compounds [25].

To determine whether **9** is a protonophore uncoupler, we used the *E. coli* inverted membrane vesicle (IMV) system, again as previously reported [6]. Results with compound **9** and the potent, known uncoupler CCCP (carbonyl cyanide *m*-chlorophenylhydrazone) are shown in Figure 5 (panels C and D) with both ATP-powered PMF generation as well as succinate/O₂-powered PMF generation. The IMVs have their ATPase on the outside of the vesicle so ATP hydrolysis through the ATPase, or succinate/O₂, drives H⁺ into the vesicles, the fluorophore ACMA (9-amino-6-chloro-2-methoxyacridine) accumulates, and its fluorescence is self-quenched (the signal goes down). Addition of CCCP or **9** collapses the PMF and fluorescence increases (back to normal). For CCCP, the EC₅₀ is 0.47 μM in ATP and 0.21 μM in succinate; for **9**, the EC₅₀ for PMF collapse is 24 μM in ATP and 28 μM in succinate, Figure 5C,D (corresponding to 8 and 9.5 μg/mL, respectively). This is relatively weak uncoupling, but could lead to inhibition of some transporters, including drug efflux pumps.

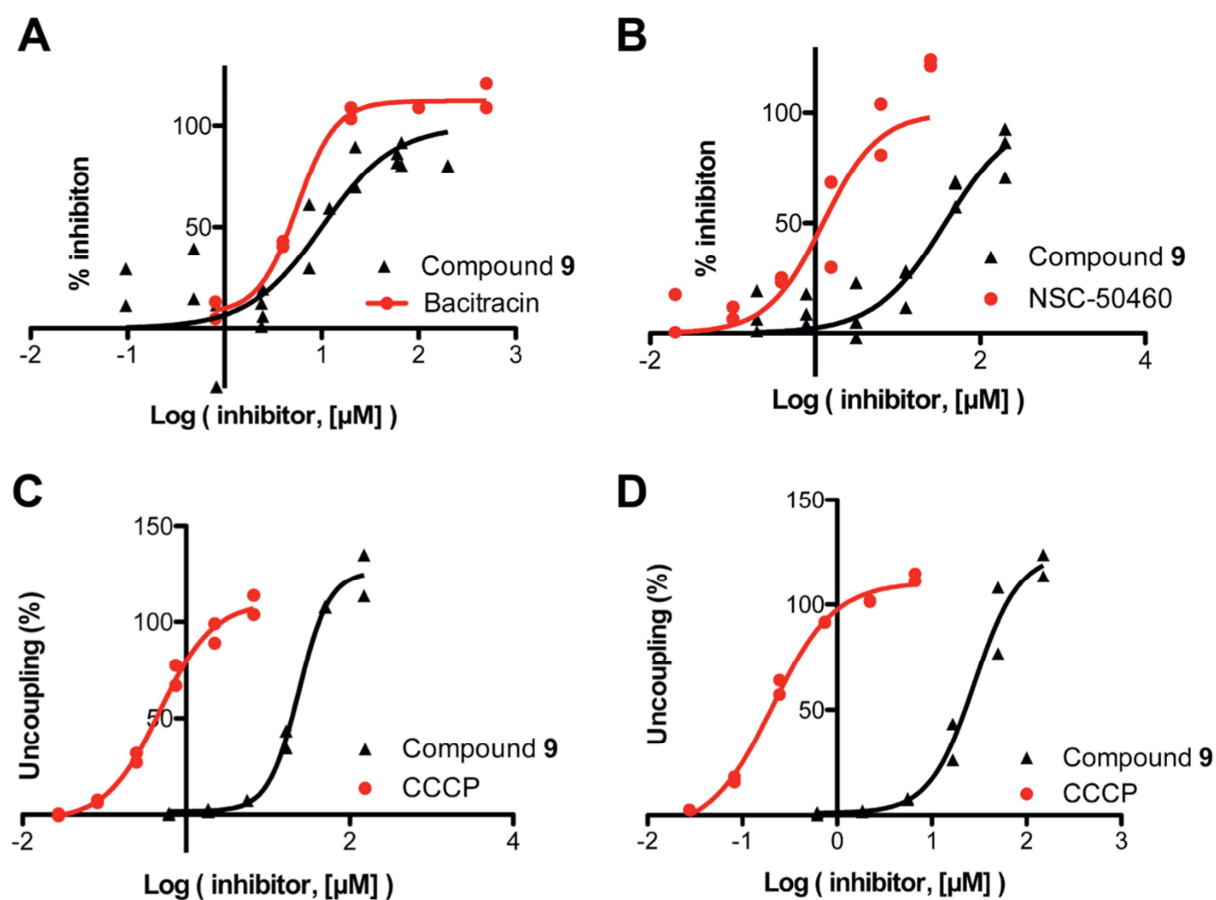


Figure 5. Dose response curves for enzyme inhibition by **9** and its effects on the PMF. A) UPPP (YubB) inhibition; bacitracin control. B) UPPS inhibition, bisamidine NSC-50460 control. (C) PMF collapse in *E. coli* IMVs, ATP driven PMF, CCCP control. (D) As C but succinate/O₂-driven PMF generation.

3.6. Resensitization of VRSA to the Effect of Vancomycin. Vancomycin is a valuable therapeutic agent for treatment of drug-resistant staphylococcal infections. However, the emergence of clinical isolates exhibiting resistance to vancomycin is of great concern. One approach we have investigated in order to try and counter vancomycin resistance is to use small molecules to resensitize VRSA to the effect of vancomycin. This approach has shown promise *in vitro*, with small molecules such as the phenylthiazole analogues [7, 19] that target the early steps in cell wall biosynthesis, formation of undecaprenyl phosphate. We thus next investigated

whether the new phenylthiazoles would be capable of re-sensitizing VRSA to the effect of vancomycin (which acts downstream of UPPS and UPPP). We tested compounds **5** (with a phenyl side-chain), **7** (with an alicyclic side-chain) and **9** (with linear side-chain), at sub-inhibitory concentration ($\frac{1}{2} \times \text{MIC}$) in combination with vancomycin against a clinical isolate of *S. aureus* (VRS10) that exhibits high-level resistance to vancomycin (MIC of 512 $\mu\text{g/mL}$). All three compounds were effective at sensitizing VRS10 to the effect of vancomycin, producing a 512-fold improvement in vancomycin's MIC value (Table 3), opening up the possibility that these or related alkynylphenylthiazoles might serve as partners to vancomycin in combating extremely drug-resistant staphylococcal infections.

Table 3. The minimum inhibitory concentration (MIC, in $\mu\text{g/mL}$) of vancomycin (VAN) in the absence and presence of a sub-inhibitory concentration ($\frac{1}{2} \times \text{MIC}$) of tested compounds against vancomycin-resistant *S. aureus* (VRS10).

VRSA strain	MIC of VAN	MIC of VAN + 5	Fold re-sensitization of VRSA to vancomycin	MIC of VAN + 7	Fold re-sensitization of VRSA to vancomycin	MIC of VAN + 9	Fold re-sensitization of VRSA to vancomycin
VRS10	512	1	512-fold	1	512-fold	1	512-fold

3.7. In vitro Pharmacokinetic Profiling. Nearly 90% of drugs currently in the drug discovery/development pipeline exhibit poor physicochemical properties such as limited aqueous solubility, poor permeability, or both [20]. The first-generation phenylthiazoles indeed exhibited a poor physicochemical profile, including limited ability to cross the gastrointestinal tract (as evaluated via the Caco-2 bidirectional permeability assay), due in large part to being a substrate for the P-gp efflux system [5a]. Additionally, first-generation phenylthiazoles containing the *n*-alkyl lipophilic tail were found to be substrates for CYP450. This resulted in very short half-lives and high clearance rates ($t_{1/2}$ of **1a** is below 30 minutes, Figure 1) [5a]. The only exception among all first-generation phenylthiazoles was the hexynyl analogue (**1b**) that possessed a longer

$t_{1/2}$ and lower clearance rate (Figure 1), but **1b** was not effective in treating a systemic MRSA infection *in vivo* [5c, 21].

To examine if the modifications made in the new series of phenylthiazoles improved the permeability and metabolic stability profiles, compound **9** and its imidazoliny analogue **19** were selected for further analysis. Initially, the permeability profile of the compounds was evaluated via the Caco-2 bidirectional permeability assay. Both compounds **9** and **19** showed low permeability through Caco-2 cells, comparable to the well-known H2 antagonist ranitidine (Table 4). The guanidiny derivative **9** was a good substrate for P-gp, with an efflux ratio of 69.

Table 4. Caco-2 bidirectional permeability analysis for compounds **9** and **19**.

Test compound	Assay Duration (minutes)	Mean A→B P_{app} (10^{-6} cm/sec)	Mean B→A P_{app} (10^{-6} cm/sec)	Efflux ratio ($P_{app(B→A)} / P_{app(A→B)}$)	P-gp substrate	Notes
Colchicine	60	0.13	5.54	44.30	Yes	
Ranitidine	60	0.27	1.71	6.30	Yes	Poor-permeability control
Labetolol	60	8.81	35.05		Yes	Moderate-permeability control
Propranolol	60	24.99	42.44	1.70	No	High-permeability control
9	60	0.05	0.35	69	Yes	Low permeability
19	60	0.13	0.13	0.96	No	Low permeability

(Table 4). Interestingly, the imidazoliny analogue **19**, which contains of fewer hydrogen bond donor (HBD) groups, was found to not be a P-gp substrate (efflux ratio < 1, similar to the control drug propranolol). Compound **19** demonstrated similar rates of permeation in both directions: from apical (A) to basolateral (B), and *vice-versa* (Table 4). This result suggests that neither

compound would be suitable to be administered orally, given their slow rate of permeation across the GI tract (simulated by the Caco-2 monolayer). Intravenous infusion of these compounds may be an alternative option, however, depending on the metabolic stability, which we thus investigated using pooled human liver microsomes. Both compounds **9** and **19** were found to have a markedly improved stability to hepatic metabolism (with a clearance rate that was $< 115.5 \mu\text{L}/\text{min}\cdot\text{mg}$) compared to the first-generation phenylthiazoles. This resulted in noticeably longer half-lives for compounds **9** and **19** of 4.8 and 8 hours, respectively (Table 5).

Table 5. Metabolic stability analysis for compounds **9** and **19** in HLM.

Test Article	Test Concentration (μM)	Mean CL_{int} ($\mu\text{L}/\text{min}\cdot\text{mg}$)	Mean $t_{1/2}$ (minutes)	Notes
Terfenadine	0.1	774.0	8.95	High clearance control
Verapamil	0.1	286.6	24.20	High clearance control
Propranolol	0.1	< 115.5	143.80	Low clearance control
Imipramine	0.1	< 115.5	87.20	Low clearance control
9	0.1	< 115.5	292.00	Stable to metabolism
19	0.1	< 115.5	476.30	Stable to metabolism

3.8. In vivo Pharmacokinetic Profiling. To further confirm that the chemical modifications made to the new generation of phenylthiazoles positively impacted their pharmacokinetic profile, naïve Sprague–Dawley rats were intravenously dosed with compound **9**. The results obtained when fit within a two-compartment model indicate a biological half-life of > 4 hours (Table 6), in agreement with the hepatic microsomal stability result described above. Taken together, these

results would permit a twice-daily dosing regimen to be used for compound **9**, if administered intravenously.

Table 6. *In vivo* PK parameters of compound **9** in rat after single IV bolus injection.

	t_{1/2} (h)	CL (L/hr)	AUC mg.hr/L	V_b (L)	V_{dss} (L)
9	4.43	5.36	0.69	18.46	5.51

t_{1/2}: half-life; CL: clearance; V_b: volume of distribution in 2nd compartment (peripheral tissues); V_{dss}: volume of distribution at the steady state

3.9. Investigating the Anti-MRSA Activity of **9** and **11** in a *C. elegans* Model of MRSA

Infection. The improvement in stability to hepatic metabolism observed with compound **9** led us to investigate its effect in treating *in vivo* MRSA infections. Compound **9**, and the rapidly-bactericidal analogue **11**, were initially evaluated in a *C. elegans* model of MRSA infection. The *C. elegans* animal model is an established system for investigating the efficacy of antibacterial agents *in vivo* in the early stages of drug discovery [22]. *C. elegans* is a useful model as it expresses cytochrome P450 enzymes that are homologous to mammalian enzymes [22]. Therefore, it permits the investigation of the pharmacodynamic effect of rapidly metabolized xenobiotics, prior to evaluating molecules in higher-order animal models. To examine the efficacy of the alkynyl-containing phenylthiazoles to reduce the burden of MRSA in infected *C. elegans*, worms were treated with compounds **9** (alicyclic-containing derivative) or **11** (linear side chain analogue). As shown in Figure 6, both compounds were as potent as vancomycin, and they reduced the burden of MRSA USA300 in infected *C. elegans* by ~90% (Figure 6). This value is almost nine times higher than the initial lead compound **1b** [24], indicating that the modifications made in this series of phenylthiazoles resulted in significantly improved efficacy.

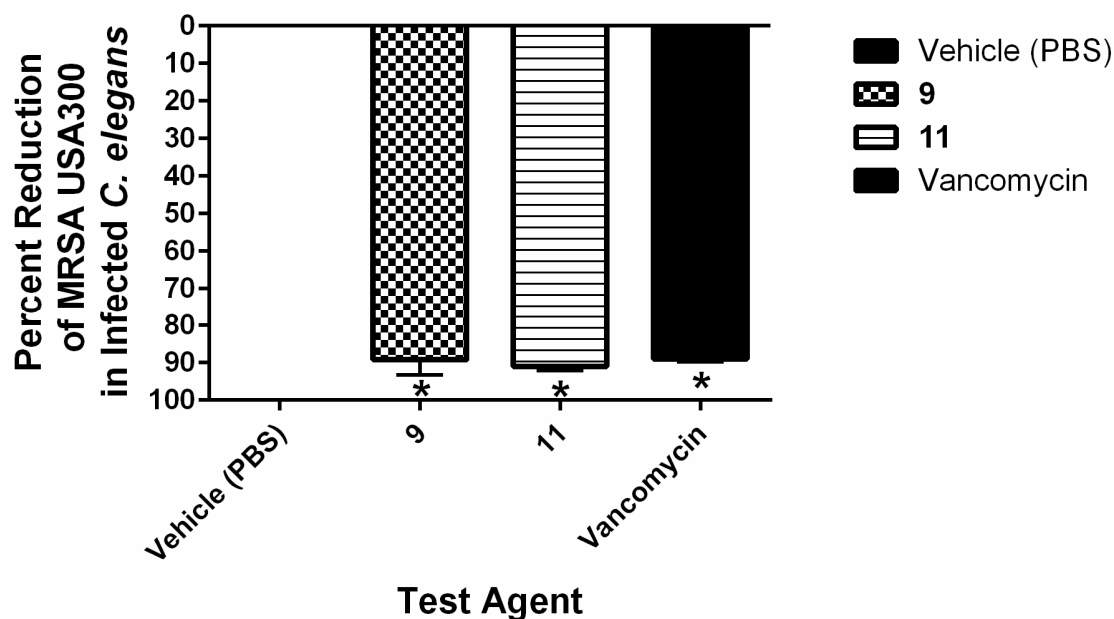


Figure 6. Antibacterial activity of 9, 11, and vancomycin *in vivo* against MRSA-infected *C. elegans*. Examination of the antibacterial activity of test agents (at 20 $\mu\text{g}/\text{mL}$) in *C. elegans* AU37 infected with methicillin-resistant *Staphylococcus aureus* USA300. Vancomycin served as a positive control. Worms (in L4 stage of growth) were infected with bacteria for six hours before transferring 25-30 worms to wells of a 96-well plate. Test agents were added and incubated with worms for 18 hours. Worms were sacrificed and the number of viable colony-forming units of MRSA USA300 in infected worms was determined for each treatment regimen. The figure presents the average percent reduction of MRSA USA300 (relative to worms receiving the negative control, PBS) for each treatment. A one-way ANOVA with post-hoc Dunnet's multiple comparisons found statistical difference between worms treated with compounds 9, 11, or vancomycin relative to the negative control (vehicle alone) (*, $P < 0.05$).

3.10. MRSA Murine Skin Infection. MRSA is a leading cause of uncomplicated (simple abscess) and complicated (infected burns and foot ulcers) skin infections in humans [25]. Treatment of uncomplicated skin infections often involves multiple doses of a topical antibiotic agent, such as fusidic acid or mupirocin [26]. Given the promising result obtained from the *C. elegans* study, we thus next moved to evaluate the effectiveness of compounds 9 and 11 in mice using an established MRSA skin infection model. Mice were injected intradermally with MRSA USA300, and an abscess formed near the injection site three days after infection. The wounds were subsequently treated twice daily (for five consecutive days) with a topical suspension of

either compounds **9**, **11**, or fusidic acid. The wounds present in one group of mice were treated with the vehicle (petroleum jelly) alone, for comparison. Compounds **9** (0.61-log_{10} , 73 % reduction) and **11** (0.58-log_{10} , 71% reduction) were found to be about as effective as the control antibiotic fusidic acid (0.71-log_{10} , 78% reduction) in reducing the burden of MRSA in the wounds of infected mice (compared to mice treated with the vehicle alone) (Figure 7). There was no excess inflammation (redness or swelling around the wound site) or toxicity observed in wounds after exposure to the compounds, or fusidic acid.

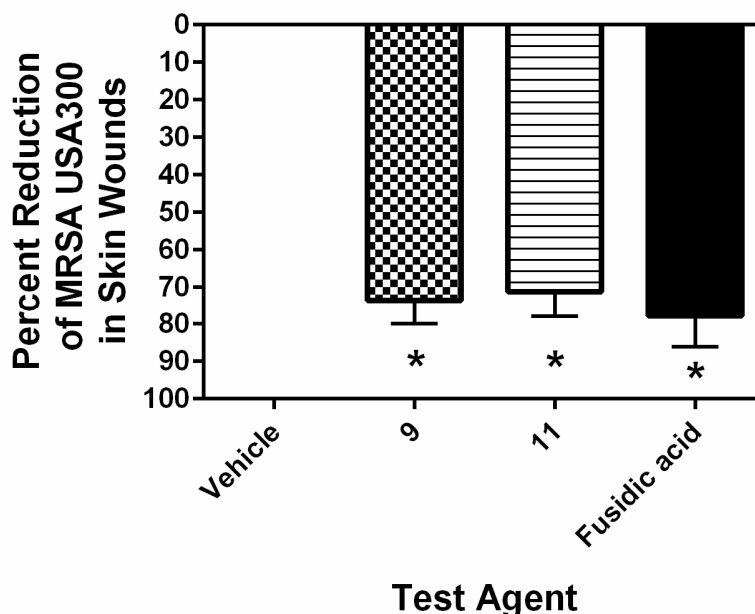


Figure 7. Reduction of MRSA USA300 in infected skin wounds of mice. Mice ($n = 5$ per group) received an intradermal injection of MRSA USA300. After formation of an abscess at the site of injection, wounds were treated twice daily (for five days) with a 2% suspension of compounds **9**, **11**, or fusidic acid (using petroleum jelly as the vehicle). Twelve hours after administering the last dose, mice were euthanized, wounds extracted and homogenized to determine the presence of MRSA in wounds. The figure presents the average percent reduction of MRSA CFU/mL in murine skin lesions. A one-way ANOVA with post-hoc Dunnet's multiple comparisons found statistical difference between mice treated with compounds **9**, **11**, or fusidic acid compared to mice receiving the vehicle (petroleum jelly) alone (*, $P < 0.05$).

3.11. Neutropenic Murine Thigh Infection Experiment. Encouraged by the previous results in *C. elegans* and the uncomplicated murine skin wound model, in addition to the *in vivo* PK study, compound **9** was tested in a systemic murine model of MRSA soft-tissue infection. Mice received an intramuscular injection of MRSA USA300 (5.35×10^6 CFU) in the right thigh. Each group of mice were treated twice (2 and 12 hours post-infection) with compound **9**, or vancomycin. Mice receiving the vehicle alone served as the negative control. Mice were humanely euthanized (24 hours post-infection) and the infected thighs were aseptically removed in order to count MRSA CFU post-treatment. Compound **9** (0.71-log_{10} , 77% reduction) was slightly more effective than the control antibiotic vancomycin (0.46-log_{10} , 66% reduction), the drug of choice for treatment of invasive MRSA infections, in reducing the burden of MRSA in the thigh of the infected mice (Figure 8). Importantly, compound **9** (20 mg/kg) achieved its effect at 40% the dose of vancomycin (50 mg/kg), further confirming the potent anti-MRSA activity of compound **9**, and its stability.

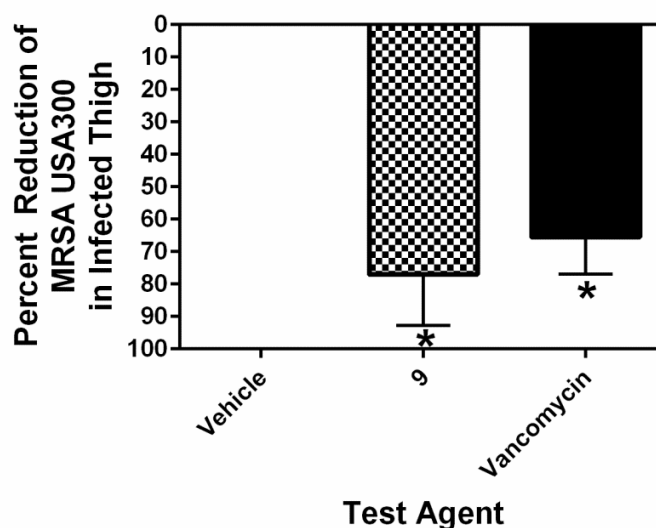


Figure 8: Reduction of MRSA USA300 in infected thigh of mice after treatment with compound 9 or vancomycin. Average percent reduction of MRSA CFU/g tissue in murine right thigh after treatment (two doses per day). A one-way ANOVA with post-hoc Dunnet's multiple

comparisons found statistical significance (*, $P < 0.05$) between mice treated with compound **9** and vancomycin compared to mice receiving the vehicle (10% DMSO, 10% Tween 80, 80% PBS) alone.

4. CONCLUSIONS

The results we have described here are of general interest since we have developed new phenylthiazole compounds that have good activity both *in vitro* and *in vivo* against methicillin-resistant *Staphylococcus aureus*. The most promising compounds killed MRSA *in vitro* at concentrations as low as 0.5 $\mu\text{g/mL}$, and were active against extracellular as well as intracellular (macrophage resident) bacteria. They act by targeting the enzymes undecaprenyl diphosphate synthase and undecaprenyl diphosphate phosphatase, involved in bacterial cell wall biosynthesis. Compound **9** was of particular interest since it had good resistance to microsomal P450 enzymes, and was active against MRSA in three animal models: *C. elegans*, a murine skin infection model, and a neutropenic murine thigh-infection model. In mice, compound **9** demonstrated comparable potency to vancomycin and at lower doses, and thus represents a new lead for the treatment of MRSA infections.

5. EXPERIMENTAL METHODS

5.1. Chemistry

5.1.1. General. ^1H NMR spectra were run at 400 MHz and ^{13}C spectra were determined at 100 MHz in deuterated chloroform (CDCl_3), or dimethyl sulfoxide ($\text{DMSO}-d_6$) on a Varian Mercury VX-400 NMR spectrometer. Chemical shifts are given in parts per million (ppm) on the delta (δ) scale. Chemical shifts were calibrated relative to those of the solvents. Flash chromatography was performed on 230-400 mesh silica. The progress of reactions was monitored with Merck silica gel IB2-F plates (0.25 mm thickness). The infrared spectra were recorded in potassium

bromide disks on pye Unicam SP 3300 and Shimadzu FT IR 8101 PC infrared spectrophotometer. Mass spectra were recorded at 70 eV. High resolution mass spectra for all ionization techniques were obtained from a FinniganMAT XL95. Melting points were determined using capillary tubes with a Stuart SMP30 apparatus and are uncorrected. All yields reported refer to isolated yields.

5.1.2. 1-(4-Methyl-2-(4-substituted alkynyl) phenyl) thiazol-5-yl) ethanone 4a-j.

General procedure: To dry DMF (5 mL) in a 25-mL sealed tube, compound **3** (500 mg, 1.45 mmol), appropriate alkynes (2.91 mmol), triethylamine (1 mL), and cesium carbonate (947 mg, 2.91 mmol) were added. After the reaction mixture was purged with dry nitrogen gas for 20 minutes, dichloro-bis(triphenylphosphine)palladium (II) (52 mg, 0.072 mmol) and copper(I) iodide (28 mg, 0.145 mmol) were added. The sealed tube was then placed in an oil bath and stirred at 65 °C for 16 hours. After cooling to room temperature, the reaction mixture was passed through celite, followed by chloroform (2×50 mL). The organic materials were then concentrated under reduced pressure. The crude materials were purified and washed via silica gel flash column chromatography using hexane-ethyl acetate (9:1). Yields, physical properties, and spectral data of isolated purified products are listed below:

5.1.2.1. 1-(4-Methyl-2-(4-phenylethynyl)phenyl)thiazol-5-yl)ethanone (4a). Yellow solid (200 mg, 43%) mp = 125 °C. ¹H NMR (CDCl₃) δ: 7.97 (d, *J* = 8.4 Hz, 2H), 7.61 (d, *J* = 8 Hz, 2H), 7.55 (d, *J* = 6.4 Hz, 2H), 7.37 (d, *J* = 6.8 Hz, 2H), 7.36 (t, *J* = 8 Hz, 1H), 2.79 (s, 3H), 2.57 (s, 3H); ¹³C NMR (CDCl₃) δ: 190.40, 168.45, 159.62, 132.22, 132.19, 131.68, 131.49, 128.68, 128.10, 127.64, 126.19, 122.78, 92.20, 88.79, 29.65, 18.64; Anal. Calc. for: C₂₀H₁₅NOS (317): C, 75.68; H, 4.76; N, 4.41%; Found: C, 75.69; H, 4.75; N, 4.40%.

5.1.2.2. 1-(2-(4-(Cyclohexylethynyl)phenyl)-4-methylthiazol-5-yl)ethanone (4b).

Yellowish oil (420 mg, 89%). ^1H NMR (CDCl_3) δ : 7.90 (d, $J = 8.4$ Hz, 2H), 7.46 (d, $J = 8.4$ Hz, 2H), 2.77 (s, 3H), 2.64 (p, $J = 8.8$ Hz, 1H), 2.56 (s, 3H), 1.90-1.25 (m, 10H); ^{13}C NMR (CDCl_3) δ : 190.40, 186.75, 159.56, 132.18, 131.46, 131.27, 127.23, 126.60, 97.73, 80.13, 32.55, 30.77, 29.68, 25.86, 24.88, 18.43; Anal. Calc. for: $\text{C}_{20}\text{H}_{21}\text{NOS}$ (323): C, 74.27; H, 6.54; N, 4.33%; Found: C, 74.25; H, 6.53; N, 4.31%.

5.1.2.3. 1-(2-(4-(Cyclopentylethynyl)phenyl)-4-methylthiazol-5-yl)ethanone (4c). Orange oil (400 mg, 89%). ^1H NMR (CDCl_3) δ : 7.89 (d, $J = 8.4$ Hz, 2H), 7.44 (d, $J = 8$ Hz, 2H), 2.84 (m, 1H), 2.76 (s, 3H), 2.55 (s, 3H), 1.77-1.24 (m, 8H); Anal. Calc. for: $\text{C}_{19}\text{H}_{19}\text{NOS}$ (309): C, 73.75; H, 6.19; N, 4.53%; Found: C, 73.73; H, 6.20; N, 4.52%.

5.1.2.3. 1-(2-(4-(Cyclopentylprop-1-yn-1-yl)phenyl)-4-methylthiazol-5-yl)ethanone (4d). Orange oil (350 mg, 74%). ^1H NMR (CDCl_3) δ : 7.97 (d, $J = 8.7$ Hz, 2H), 7.51 (d, $J = 8.7$ Hz, 2H), 2.70 (s, 3H), 2.57 (s, 3H), 2.49 (dd, $J = 1.8$ Hz, $J = 6.6$ Hz, 2H), 1.79 (m, 1H), 1.56-1.30 (m, 8H); ^{13}C NMR (CDCl_3) δ : 190.40, 168.96, 159.55, 132.14, 131.42, 131.35, 127.28, 126.59, 97.95, 79.69, 33.80, 30.27, 25.07, 20.92, 18.41, 13.64; Anal. Calc. for: $\text{C}_{20}\text{H}_{21}\text{NOS}$ (323): C, 74.27; H, 6.54; N, 4.33%; Found: C, 74.28; H, 6.52; N, 4.32%.

5.1.2.4. 1-(2-(4-(Cyclopropylethynyl)phenyl)-4-methylthiazol-5-yl)ethanone (4e). Pale yellow oil (360 mg, 88%). ^1H NMR (CDCl_3) δ : 7.89 (d, $J = 8$ Hz, 2H), 7.44 (d, $J = 8.4$ Hz, 2H), 2.77 (s, 3H), 2.56 (s, 3H), 1.64 (p, $J = 6.8$ Hz, 1H), 1.49 (q, $J = 8.4$ Hz, 2H), 1.39 (q, $J = 5.2$ Hz, 2H); ^{13}C NMR (CDCl_3) δ : 190.42, 168.71, 159.57, 132.15, 131.48, 131.35, 127.02, 126.63, 96.80, 78.15, 19.04, 13.64, 8.72, 0.28; Anal. Calc. for: $\text{C}_{17}\text{H}_{15}\text{NOS}$ (281): C, 72.57; H, 5.37; N, 4.98%; Found: C, 72.56; H, 5.38; N, 4.99%.

5.1.2.5. 1-(4-Methyl-2-(4-(pent-1-yn-1-yl)phenyl)thiazol-5-yl)ethanone (4f). Yellow oil (370 mg, 90%). ^1H NMR (CDCl_3) δ : 7.91 (d, $J = 8.4$ Hz, 2H), 7.47 (d, $J = 8.4$ Hz, 2H), 2.77 (s,

3H), 2.56 (s, 3H), 2.43 (t, $J = 6.9$ Hz, 2H), 1.69 (m, 2H), 1.07 (t, $J = 7.8$ Hz, 3H); ^{13}C NMR (CDCl_3) δ : 190.42, 168.72, 159.56, 132.16, 131.54, 131.31, 127.15, 126.64, 93.56, 80.30, 30.76, 22.07, 21.51, 18.42, 13.64; Anal. Calc. for: $\text{C}_{17}\text{H}_{17}\text{NOS}$ (283): C, 72.05; H, 6.05; N, 4.94%; Found: C, 72.06; H, 6.07; N, 4.95%.

5.1.2.6. 1-(2-(4-(Hept-1-yn-1-yl)phenyl)-4-methylthiazol-5-yl)ethanone (4g). Yellow oil (350 mg, 78%). ^1H NMR (CDCl_3) δ : 7.91 (d, $J = 8$ Hz, 2H), 7.47 (d, $J = 8$ Hz, 2H), 2.77 (s, 3H), 2.56 (s, 3H), 2.40 (t, $J = 7.2$ Hz, 2H), 1.64 (p, $J = 6.8$ Hz, 2H), 1.47 (m, 4H), 0.90 (t, $J = 5.6$ Hz, 3H); ^{13}C NMR (CDCl_3) δ : 190.40, 168.72, 159.56, 132.14, 131.52, 131.30, 127.18, 126.64, 93.81, 80.15, 31.33, 29.68, 28.61, 28.57, 22.53, 19.55, 18.42, 14.04; Anal. Calc. for: $\text{C}_{19}\text{H}_{21}\text{NOS}$ (311): C, 73.27; H, 6.80; N, 4.50%; Found: C, 73.26; H, 6.81; N, 4.52%.

5.1.2.7. 1-(4-Methyl-2-(4-(oct-1-yn-1-yl)phenyl)thiazol-5-yl)ethanone (4h). Yellow oil (385 mg, 81%). ^1H NMR (CDCl_3) δ : 7.90 (d, $J = 8$ Hz, 2H), 7.46 (d, $J = 8.4$ Hz, 2H), 2.77 (s, 3H), 2.56 (s, 3H), 2.44 (t, $J = 7.2$ Hz, 2H), 1.65 (p, $J = 7.2$ Hz, 2H), 1.47 (m, 6H), 0.94 (t, $J = 9.6$ Hz, 3H); ^{13}C NMR (CDCl_3) δ : 190.40, 168.72, 159.56, 132.14, 131.52, 131.30, 127.18, 126.64, 93.81, 80.15, 31.33, 30.53, 29.68, 28.61, 28.57, 22.53, 19.55, 18.42, 14.04; Anal. Calc. for: $\text{C}_{20}\text{H}_{23}\text{NOS}$ (325): C, 73.81; H, 7.12; N, 4.30%; Found: C, 73.82; H, 7.13; N, 4.29%.

5.1.2.8. 1-(2-[4-(3,3-Dimethylbut-1-yn-1-yl)phenyl]-4-methylthiazol-5-yl)ethanone (4i). Faint yellow oil (351 mg, 80%). ^1H NMR (CDCl_3) δ : 7.90 (d, $J = 8$ Hz, 2H), 7.45 (d, $J = 7.6$ Hz, 2H), 2.77 (s, 3H), 2.56 (s, 3H), 1.33 (s, 9H); ^{13}C NMR (CDCl_3) δ : 190.41, 168.97, 159.53, 132.17, 131.42, 131.26, 127.20, 126.59, 101.72, 78.67, 30.88, 19.04, 18.43, 13.65; Anal. Calc. for: $\text{C}_{18}\text{H}_{19}\text{NOS}$ (297): C, 72.69; H, 6.44; N, 4.71%; Found: C, 72.68; H, 6.46; N, 4.70%.

5.1.2.9. 1-(2-(4-(3-Amino-3-methylbut-1-yn-1-yl)phenyl)-4-methylthiazol-5-yl)ethanone (4j). Faint yellow oil (300 mg, 69%). ^1H NMR (CDCl_3) δ : 8.01 (brs, 2H), 7.91 (d, $J = 8$ Hz, 2H), 7.46 (d, $J = 8.4$ Hz, 2H), 2.94 (s, 3H), 2.87 (s, 3H), 2.77 (s, 3H), 2.56 (s, 3H); ^{13}C NMR (CDCl_3)

δ : 190.40, 168.98, 159.53, 132.17, 131.42, 131.26, 127.20, 126.59, 101.72, 78.67, 30.88, 29.04, 19.07, 18.43, 13.65; Anal. Calc. for: C₁₇H₁₈N₂OS (298): C, 68.43; H, 6.08; N, 9.39%; Found: C, 68.42; H, 6.07; N, 9.40%.

5.1.3. 2-(1-(2-(4-Substituted)phenyl)-4-methylthiazol-5-yl)ethylidene)hydrazine-1-carboximidamide (5-14).

General procedure: Method A: Thiazole derivatives **4a-j** (0.63 mmol) were dissolved in absolute ethanol (10 mL), aminoguanidine hydrochloride (340 mg, 3.15 mmol), a catalytic amount of anhydrous LiCl (5 mg), and (0.5 mL) glacial acetic acid. The reaction mixture was heated at reflux for 24 hours and the solvent was concentrated under reduced pressure and then poured on crushed ice. The formed precipitated solid was collected by filtration and washed with copious amount of water. Crystallization from absolute ethanol afforded the desired products as solids.

Method B: Thiazole derivatives **4a-j** (0.63 mmol) were dissolved in absolute ethanol (10 mL), aminoguanidine hydrochloride (70 mg, 0.63 mmol), and hydrochloric acid (0.1 mL). The reaction mixture was heated at reflux for four hours. The solvent was concentrated under reduced pressure, poured onto crushed ice, and neutralized with sodium hydroxide (to pH 7-8). The solid precipitate was collected by filtration and washed with copious amount of water. Crystallization from absolute ethanol afforded the desired products, as solids.

5.1.3.1. 2-(1-(2-(4-Phenylethynyl)phenyl)-4-methylthiazol-5-yl)ethylidene)hydrazine-1-carboximidamide (5). Yellow solid (205 mg, 87%): mp = 190-192 °C. ¹H NMR (DMSO-*d*₆) δ : 11.19 (brs, 1H), 7.98 (d, *J* = 8.9 Hz, 2H), 7.70 (d, *J* = 8.7 Hz, 2H), 7.58 (d, *J* = 8 Hz, 2H), 7.46 (m, 3H), 7.44 (brs, 3H), 2.63 (s, 3H), 2.43 (s, 3H). ¹³C NMR (DMSO-*d*₆) δ : 163.68, 155.96, 152.42, 146.94, 132.37, 132.08, 131.32, 128.96, 128.68, 126.08, 124.06, 121.86, 121.86, 91.48,

88.73, 17.95, 17.90; HRMS (EI) m/z 373.1358 M^+ , calc. for $C_{21}H_{19}N_5S$ 373.1361; Anal. Calc. for: $C_{21}H_{19}N_5S$ (373): C, 67.54; H, 5.13; N, 18.75%; Found: C, 67.55; H, 5.12; N, 18.74%.

5.1.3.2. 2-(1-(2-(4-(Cyclohexylethynyl)phenyl)-4-methylthiazol-5-yl)ethylidene)hydrazine-1-carboximidamide (6). Yellow-white solid (196 mg, 84%): mp = 153-154 °C. 1H NMR (DMSO- d_6) δ : 11.37 (brs, 1H), 7.89 (d, J = 8.4 Hz, 2H), 7.87 (brs, 1H), 7.70 (brs, 2H), 7.50 (d, J = 8.4 Hz, 2H), 2.65 (m, 1H), 2.61 (s, 3H), 2.43 (s, 3H). 1.81-1.32 (m, 10H); ^{13}C NMR (DMSO- d_6) δ : 163.98, 155.90, 152.53, 147.03, 131.99, 131.63, 130.98, 125.97, 125.22, 96.99, 80.12, 32.02, 28.81, 25.28, 24.20, 18.13, 18.04; HRMS (EI) m/z 379.1838 M^+ , calc. for $C_{21}H_{25}N_5S$ 379.1831; Anal. Calc. for: $C_{21}H_{25}N_5S$ (379): C, 66.46; H, 6.64; N, 18.45%; Found: C, 66.45; H, 6.64; N, 18.44%.

5.1.3.3. 2-{1-[2-(4-(Cyclopentylethynyl)phenyl)-4-methylthiazol-5-yl]ethylidene}hydrazine-1-carboximidamide (7). Yellowish solid (195 mg, 82%): mp = 143-144 °C. 1H NMR (DMSO- d_6) δ : 11.25 (brs, 1H), 7.93 (brs, 1H), 7.88 (d, J = 8.4 Hz, 2H), 7.60 (brs, 2H), 7.48 (d, J = 8.1 Hz, 2H), 2.89 (m, 1H), 2.61 (s, 3H), 2.41 (s, 3H). 1.99-1.56 (m, 8H); ^{13}C NMR (DMSO- d_6) δ : 168.07, 164.09, 158.33, 152.62, 148.45, 131.54, 126.50, 125.90, 120.38, 97.30, 79.56, 33.33, 29.95, 24.50, 18.36, 17.95; HRMS (EI) m/z 365.1685 M^+ , calc. for $C_{20}H_{23}N_5S$ 365.1674; Anal. Calc. for: $C_{20}H_{23}N_5S$ (365): C, 65.72; H, 6.34; N, 19.16%; Found: C, 65.71; H, 6.33; N, 19.17%.

5.1.3.4. 2-(1-(2-(4-(3-Cyclopentylprop-1-yn-1-yl)phenyl)-4-methylthiazol-5-yl)ethylidene)hydrazine-1-carboximidamide (8). Yellowish brown solid (175 mg, 74%): mp = 140-141 °C. 1H NMR (DMSO- d_6) δ : 11.27 (brs, 1H), 7.93 (brs, 1H), 7.89 (d, J = 8.4 Hz, 2H), 7.68 (brs, 2H), 7.51 (d, J = 8.7 Hz, 2H), 2.62 (s, 3H), 2.48 (dd, J = 3.6 Hz, J = 6.9 Hz, 2H), 2.43 (s, 3H), 1.81 (m, 1H), 1.56-1.30 (m, 8H). ^{13}C NMR (DMSO- d_6) δ : 163.98, 155.89, 152.52, 147.04, 132.01, 131.01, 126.00, 125.30, 120.62, 92.78, 80.18, 31.47, 24.72, 24.40, 18.45, 18.10, 13.41;

HRMS (EI) m/z 379.1833 M^+ , calc. for $C_{21}H_{25}N_5S$ 379.1831; Anal. Calc. for: $C_{21}H_{25}N_5S$ (379): C, 66.46; H, 6.64; N, 18.45%; Found: C, 66.45; H, 6.63; N, 18.46%.

5.1.3.5. 2-(1-(2-(4-(Cyclopropylethynyl)phenyl)-4-methylthiazol-5-yl)ethylidene)hydrazine-1-carboximidamide (9). Yellowish solid (184 mg, 76%): mp = 164-165 °C. 1H NMR (DMSO- d_6) δ : 11.55 (brs, 1H), 7.87 (d, J = 8.7 Hz, 2H), 7.77 (brs, 3H), 7.47 (d, J = 8.4 Hz, 2H), 2.60 (s, 3H), 2.43 (s, 3H), 1.62 (m, 1H), 0.92 (q, J = 8.1 Hz, 2H), 0.77 (q, J = 2.4 Hz, 2H), ^{13}C NMR (DMSO- d_6) δ : 168.07, 163.98, 155.87, 152.52, 147.05, 132.01, 131.54, 125.96, 125.21, 120.42, 96.58, 75.16, 18.45, 18.07, 13.41, 8.53; HRMS (EI) m/z 337.1352 M^+ , calc. for $C_{18}H_{19}N_5S$ 337.1361; Anal. Calc. for: $C_{18}H_{19}N_5S$ (337): C, 64.07; H, 5.68; N, 20.75%; Found: C, 64.05; H, 5.67; N, 20.76%.

5.1.3.6. 2-(1-(4-Methyl-2-(4-(pent-1-yn-1-yl)phenyl)thiazol-5-yl)ethylidene)hydrazine-1-carboximidamide (10). Yellowish solid (195 mg, 82%): mp = 176-178 °C. 1H NMR (DMSO- d_6) δ : 11.34 (brs, 1H), 7.89 (d, J = 8.4 Hz, 2H), 7.68 (brs, 3H), 7.51 (d, J = 8.7 Hz, 2H), 2.61 (s, 3H), 2.49 (t, J = 10.5 Hz, 2H), 2.43 (s, 3H), 1.61 (m, J = 7.5 Hz, 2H), 1.05 (t, J = 7.5 Hz, 3H); ^{13}C NMR (DMSO- d_6) δ : 163.96, 155.89, 152.49, 147.05, 131.96, 131.64, 125.97, 125.24, 120.43, 93.16, 80.23, 21.47, 20.59, 18.07, 17.98, 13.22; HRMS (EI) m/z 339.1520 M^+ , calc. for $C_{18}H_{21}N_5S$ 339.1518; Anal. Calc. for: $C_{18}H_{21}N_5S$ (339): C, 63.69; H, 6.24; N, 20.63%; Found: C, 63.68; H, 6.23; N, 20.63%.

5.1.3.7. 2-(1-(2-(4-(Hep-1-yn-1-yl)phenyl)-4-methylthiazol-5-yl)ethylidene)hydrazine-1-carboximidamide (11). Yellowish solid (195 mg, 82%): mp = 175-177 °C. 1H NMR (DMSO- d_6) δ : 11.20 (brs, 1H), 7.89 (d, J = 8.7 Hz, 2H), 7.56 (brs, 3H), 7.51 (d, J = 8.7 Hz, 2H), 2.61 (s, 3H), 2.49 (t, J = 8.2 Hz, 2H), 2.42 (s, 3H), 1.56 (p, J = 6.9 Hz, 2H), 1.36 (m, 4H), 0.89 (t, J = 6.6 Hz, 3H); ^{13}C NMR (DMSO- d_6) δ : 163.96, 155.99, 152.78, 147.05, 131.88, 131.63, 125.97, 125.24,

120.43, 93.17, 80.24, 30.58, 27.90, 21.83, 18.60, 18.63, 17.93, 13.71; MS (m/z); 367.24 (M^+ , 85.35%); HRMS (EI) m/z 367.1834 M^+ , calc. for $C_{20}H_{25}N_5S$ 367.1831; Anal. Calc. for: $C_{20}H_{25}N_5S$ (367): C, 65.36; H, 6.86; N, 19.06%; Found: C, 65.37; H, 6.87; N, 19.05%.

5.1.3.8. 2-(1-(4-Methyl-2-(4-oct-1-yn-1-yl)phenyl)thiazol-5-yl)ethylidene)hydrazine-1-carboximidamide (12). Yellowish brown powder (215 mg, 86%): mp = 150-151 °C. 1H NMR (DMSO- d_6) δ : 11.22 (brs, 1H), 7.89 (d, J = 8.1 Hz, 2H), 7.55 (brs, 3H), 7.50 (d, J = 8.4 Hz, 2H), 2.62 (s, 3H), 2.49 (t, J = 8.2 Hz, 2H), 2.42 (s, 3H), 1.55 (p, J = 6.3 Hz, 2H), 1.42 (m, 6H), 0.88 (t, J = 6.6 Hz, 3H); ^{13}C NMR (DMSO- d_6) δ : 163.99, 155.99, 152.98, 147.09, 131.88, 131.63, 125.92, 125.21, 120.79, 93.27, 80.04, 30.58, 27.90, 27.81, 21.83, 18.60, 18.36, 17.93, 13.71; HRMS (EI) m/z 381.1986 M^+ , calc. for $C_{21}H_{27}N_5S$ 381.1987; Anal. Calc. for: $C_{21}H_{27}N_5S$ (381): C, 66.11; H, 7.13; N, 18.36%; Found: C, 66.12; H, 7.37; N, 18.35%.

5.1.3.9. 2-(1-(2-(4-(3,3-Dimethylbut-1-yn-1-yl)-phenyl)-4-methylthiazol-5-yl)ethylidene)hydrazine-1-carboximidamide (13). Brown solid (195 mg, 82%): mp = 140-142 °C. 1H NMR (DMSO- d_6) δ : 11.42 (brs, 1H), 7.89 (d, J = 8.7 Hz, 2H), 7.70 (brs, 1H), 7.69 (brs, 2H), 7.48 (d, J = 8.7 Hz, 2H), 2.61 (s, 3H), 2.43 (s, 3H), 1.30 (s, 9H); ^{13}C NMR (DMSO- d_6) δ : 164.52, 156.31, 153.06, 147.65, 132.51, 131.54, 127.16, 126.51, 125.62, 101.60, 79.06, 30.93, 28.17, 18.51, 13.53; MS (m/z); 353.55 (M^+ , 0.75%); HRMS (EI) m/z 353.1674 M^+ , calc. for $C_{19}H_{23}N_5S$ 353.1674; Anal. Calc. for: $C_{19}H_{23}N_5S$ (353): C, 64.56; H, 6.56; N, 19.81%; Found: C, 64.57; H, 6.57; N, 19.80%.

5.1.3.10. 2-(1-(2-(4-(3-Amino-3-methylbut-1-yn-1-yl)-phenyl)-4-methylthiazol-5-yl)ethylidene)hydrazine-1-carboximidamide (14). Yellowish brown solid (197 mg, 82.5%): mp = 126-128 °C. 1H NMR (DMSO- d_6) δ : 7.91 (brs, 1H), 7.86 (d, J = 8.1 Hz, 2H), 7.62 (brs, 3H), 7.44 (d, J = 7.8 Hz, 2H), 5.82 (brs, 2H), 2.56 (s, 3H), 2.31 (s, 3H), 1.39 (s, 6H); ^{13}C NMR (DMSO- d_6)

δ : 164.12, 156.41, 153.13, 147.47, 132.68, 132.14, 129.36, 126.73, 123.32, 92.14, 83.66, 48.08, 27.88, 18.55, 13.53; MS (m/z); 354.46 (M^+ , 92%); HRMS (EI) m/z 354.1627 M^+ , calc. for $C_{18}H_{22}N_6S$ 354.1627; Anal. Calc. for: $C_{18}H_{22}N_6S$ (354): C, 60.99; H, 6.26; N, 23.71%; Found: C, 60.99; H, 6.27; N, 23.70%.

5.1.4. 2-(4-(Substitutedalkynyl)phenyl)-5-(1-(2-(4,5-dihydro-1-*H*-imidazol-2-yl)hydrazono) ethyl)-4-methylthiazole (15-24).

General procedure: Method A: Thiazole derivatives **4a-j** (0.63 mmol) were dissolved in absolute ethanol (10 mL), 2-hydrazino-2-imidazoline hydrobromide (17 mg, 0.95 mmol), a catalytic amount of anhydrous LiCl (5 mg), and 0.5 mL glacial acetic acid. The reaction mixture was heated at reflux for 24 hours. The solvent was concentrated under reduced pressure and poured onto crushed ice. The formed solid precipitate was collected by filtration and washed with copious amount of water. Crystallization from absolute ethanol afforded the desired products as solids.

Method B: Thiazole derivatives **4a-j** (0.63 mmol) were dissolved in absolute ethanol (10 mL), 2-hydrazinyl-4,5-dihydro-1*H*-imidazole hydrobromide (11.5 mg, 0.63 mmol), and hydrochloric acid (0.1 mL). The reaction mixture was heated at reflux for four hours. The solvent was concentrated under reduced pressure, poured onto crushed ice, and neutralized with sodium hydroxide (to pH 7-8). The solid precipitate was collected by filtration and washed with copious amount of water. Crystallization from absolute ethanol afforded the desired products as solids.

5.1.4.1. 5-(1-(2-(4,5-Dihydro-1*H*-imidazol-2-yl)hydrazono)ethyl)-4-methyl-2-(4-(phenylethynyl) phenyl)thiazole (15). Yellow solid (222 mg, 88%): mp = 188-190 °C. 1H NMR (DMSO- d_6) δ : 11.86 (brs, 1H), 8.07 (d, J = 8.7 Hz, 2H), 7.97 (d, J = 8.4 Hz, 2H), 7.71 (brs, 1H), 7.70 (d, J = 8.7 Hz, 2H), 7.58 (d, J = 7.5 Hz, 2H), 7.44 (t, J = 6.3 Hz 1H), 3.72 (s, 4H), 2.72 (s,

3H), 2.42 (s, 3H). ^{13}C NMR (DMSO- d_6) δ : 163.68, 155.96, 152.42, 146.42, 132.32, 132.08, 131.36, 128.96, 128.68, 126.08, 124.06, 121.86, 120.44, 91.48, 88.73, 42.93, 17.95, 17.90; HRMS (EI) m/z 399.1530 M^+ , calc. for $\text{C}_{23}\text{H}_{21}\text{N}_5\text{S}$ 399.1518; Anal. Calc. for: $\text{C}_{23}\text{H}_{21}\text{N}_5\text{S}$ (399): C, 69.15; H, 5.30; N, 17.53%; Found: C, 69.16; H, 5.31; N, 17.52%.

5.1.4.2. 2-(4-(Cyclohexylethynyl)phenyl)-5-(1-(2-(4,5-dihydro-1H-imidazol-2-yl)hydrazono) ethyl)-4-methylthiazole (16). Yellow solid (222 mg, 88%): mp = 137-139 °C. ^1H NMR (DMSO- d_6) δ : 7.97 (d, J = 8.4 Hz, 2H), 7.88 (d, J = 8.7 Hz, 2H), 7.51 (brs, 1H), 7.50 (brs, 1H), 3.67 (s, 4H), 2.71 (s, 3H), 2.38 (s, 3H), 1.82-1.23 (m, 11H); ^{13}C NMR (DMSO- d_6) δ : 167.56, 163.66, 158.15, 151.92, 147.73, 132.04, 126.56, 125.12, 120.24, 96.94, 80.13, 42.75, 32.01, 31.21, 28.08, 25.26, 24.18, 17.58; HRMS (EI) m/z 405.1997 M^+ , calc. for $\text{C}_{23}\text{H}_{27}\text{N}_5\text{S}$ 405.1987; Anal. Calc. for: $\text{C}_{23}\text{H}_{27}\text{N}_5\text{S}$ (405): C, 68.12; H, 6.71; N, 17.27%; Found: C, 68.13; H, 6.72; N, 17.26%.

5.1.4.3. 2-(4-(Cyclopentylethynyl)phenyl)-5-(1-(2-(4,5-dihydro-1H-imidazol-2-yl)hydrazono) ethyl)-4-methylthiazole (17). Yellowish solid (215 mg, 85%): mp = 144-145 °C. ^1H NMR (DMSO- d_6) δ : 12.15 (brs, 1H), 8.25 (brs, 1H), 7.86 (d, J = 8.1 Hz, 2H), 7.48 (d, J = 8.1 Hz, 2H), 3.72 (s, 4H), 2.85 (m, 1H), 2.61 (s, 3H), 2.43 (s, 3H). 1.59-1.21 (m, 8H). ^{13}C NMR (DMSO- d_6) δ : 164.09, 158.10, 152.62, 148.45, 131.54, 126.50, 125.90, 120.45, 97.30, 79.56, 42.87, 33.33, 30.31, 29.68, 24.53, 18.40, 13.34; HRMS (EI) m/z 391.1831 M^+ , calc. for $\text{C}_{22}\text{H}_{25}\text{N}_5\text{S}$ 391.1833; Anal. Calc. for: $\text{C}_{22}\text{H}_{25}\text{N}_5\text{S}$ (391): C, 67.49; H, 6.44; N, 17.89%; Found: C, 67.48; H, 6.43; N, 17.88%.

5.1.4.4. 2-(4-(Cyclopentylprop-1-yn-1-yl)phenyl)-5-(1-(2-(4,5-dihydro-1H-imidazol-2-yl)hydrazono)ethyl)-4-methylthiazole (18). Brown solid (175 mg, 74%): mp = 132-134 °C. ^1H NMR (DMSO- d_6) δ : 7.94 (brs, 1H), 7.92 (brs, 1H), 7.86 (d, J = 8.1 Hz, 2H), 7.49 (d, J = 8.1 Hz,

2H), 3.66 (s, 4H), 2.69 (s, 3H), 2.46 (dd, $J = 1.8$ Hz, $J = 6.6$ Hz, 2H), 2.39 (s, 3H), 1.62-1.30 (m, 9H). ^{13}C NMR (DMSO- d_6) δ : 168.01, 163.53, 159.50, 151.74, 147.52, 131.97, 131.73, 126.51, 125.84, 92.61, 80.15, 42.69, 31.43, 29.95, 24.68, 18.05, 17.52, 13.33; HRMS (EI) m/z 405.1993 M^+ , calc. for $\text{C}_{23}\text{H}_{27}\text{N}_5\text{S}$ 405.1987; Anal. Calc. for: $\text{C}_{23}\text{H}_{27}\text{N}_5\text{S}$ (405): C, 68.12; H, 6.71; N, 17.27%; Found: C, 68.13; H, 6.72; N, 17.26%.

5.1.4.5. 2-(4-(Cyclopropylethynyl)phenyl)-5-(1-(2-(4,5-dihydro-1H-imidazol-2-yl)hydrazono)ethyl)-4-methylthiazole (19). Yellow-green solid (221 mg, 81%): mp = 152-153 °C. ^1H NMR (DMSO- d_6) δ : 11.75 (brs, 1H), 8.15 (brs, 1H), 7.87 (d, $J = 8.4$ Hz, 2H), 7.49 (d, $J = 8.1$ Hz, 2H), 3.71 (s, 4H), 2.62 (s, 3H), 2.40 (s, 3H), 1.59 (p, $J = 6.8$ Hz, 1H), 0.90 (q, $J = 8.1$ Hz, 2H), 0.69 (q, $J = 8.1$ Hz, 2H), ^{13}C NMR (DMSO- d_6) δ : 168.11, 164.07, 158.42, 152.59, 148.47, 132.04, 130.99, 125.95, 120.61, 96.62, 85.82, 42.88, 18.44, 18.09, 17.88, 13.41, 8.53; HRMS (EI) m/z 363.1511 M^+ , calc. for $\text{C}_{20}\text{H}_{21}\text{N}_5\text{S}$ 363.1518; Anal. Calc. for: $\text{C}_{20}\text{H}_{21}\text{N}_5\text{S}$ (363): C, 66.09; H, 5.82; N, 19.27%; Found: C, 66.10; H, 5.83; N, 19.26%.

5.1.4.6. 5-(1-(2-(4,5-Dihydro-1H-imidazol-2-yl)hydrazono)ethyl)-4-methyl-2-(4-(pent-1-yn-1-yl)phenyl)thiazole (20). Yellow powder (215 mg, 83%): mp = 160-161 °C. ^1H NMR (DMSO- d_6) δ : 8.02 (brs, 1H), 7.98 (brs, 1H), 7.88 (d, $J = 8.4$ Hz, 2H), 7.51 (d, $J = 8.4$ Hz, 2H), 3.67 (s, 4H), 2.61 (s, 3H), 2.57 (t, $J = 10.5$ Hz, 2H), 2.40 (s, 3H), 1.59 (m, 2H), 1.03 (t, $J = 7.2$ Hz, 3H); ^{13}C NMR (DMSO- d_6) δ : 163.96, 155.89, 152.49, 147.05, 131.96, 131.64, 125.97, 125.24, 120.39, 93.16, 80.23, 42.69, 21.47, 20.59, 18.07, 17.98, 13.22; HRMS (EI) m/z 365.1685 M^+ , calc. for $\text{C}_{20}\text{H}_{23}\text{N}_5\text{S}$ 365.1674; Anal. Calc. for: $\text{C}_{20}\text{H}_{23}\text{N}_5\text{S}$ (365): C, 65.72; H, 6.34; N, 19.16%; Found: C, 65.73; H, 6.33; N, 19.15%.

5.1.4.7. 5-(1-(2-(4,5-Dihydro-1H-imidazol-2-yl)hydrazono)ethyl)-2-(4-(hept-1-yn-1-yl)phenyl)-4-methylthiazole (21). Brown powder (215 mg, 85%): mp = 137-139 °C. ^1H NMR

(DMSO- d_6) δ : 11.20 (brs, 1H), 7.98 (brs, 1H), 7.89 (d, $J = 8.7$ Hz, 2H), 7.51 (d, $J = 8.7$ Hz, 2H), 3.67 (s, 4H), 2.61 (s, 3H), 2.49 (t, $J = 7.2$ Hz, 2H), 2.41 (s, 3H), 1.56-1.36 (m, 6H), 0.89 (t, $J = 9.6$ Hz, 3H); ^{13}C NMR (DMSO- d_6) δ : 172.45, 164.28, 158.67, 148.35, 132.51, 131.64, 127.82, 126.43, 125.70, 93.35, 80.63, 43.31, 31.22, 28.47, 22.48, 19.20, 18.61, 14.35, 13.87; MS (m/z); 393.55 (M^+ , 76.35%); HRMS (EI) m/z 393.1984 M^+ , calc. for $\text{C}_{22}\text{H}_{27}\text{N}_5\text{S}$ 393.1987; Anal. Calc. for: $\text{C}_{22}\text{H}_{27}\text{N}_5\text{S}$: C, 67.14; H, 6.92; N, 17.80%; Found: C, 67.12; H, 6.90; N, 17.11%.

5.1.4.8. 5-(1-(2-(4,5-Dihydro-1H-imidazol-2-yl)hydrazono)ethyl)-4-methyl-2-(4-(oct-1-yn-1-yl)phenyl)thiazole (22). Brown powder (215 mg, 86%): mp = 135-137 °C. ^1H NMR (DMSO- d_6) δ : 11.55 (brs, 1H), 8.13 (brs, 1H), 7.89 (d, $J = 8.1$ Hz, 2H), 7.51 (d, $J = 8.4$ Hz, 2H), 3.72 (s, 4H), 2.62 (s, 3H), 2.49 (t, $J = 8.2$ Hz, 2H), 2.39 (s, 3H), 1.62-1.30 (m, 8H), 0.90 (t, $J = 6.6$ Hz, 3H); ^{13}C NMR (DMSO- d_6) δ : 169.05, 164.28, 158.67, 148.35, 132.47, 131.65, 127.07, 126.63, 125.70, 93.35, 80.63, 43.31, 31.22, 30.23, 28.47, 22.48, 19.20, 18.61, 14.35, 13.87; MS (m/z); 407.26 (M^+ , 92.97%); HRMS (EI) m/z 407.2148 M^+ , calc. for $\text{C}_{23}\text{H}_{29}\text{N}_5\text{S}$ 407.2144; Anal. Calc. for: $\text{C}_{23}\text{H}_{29}\text{N}_5\text{S}$: C, 67.78; H, 7.17; N, 17.18%; Found: C, 67.79; H, 7.19; N, 17.17%.

5.1.4.9. 5-(1-(2-(4,5-Dihydro-1H-imidazol-2-yl)hydrazono)ethyl)-2-(4-(3,3-dimethylbut-1-yn-1-yl)phenyl)-4-methylthiazole (23). Yellowish solid (197 mg, 77%): mp = 124-126 °C. ^1H NMR (CDCl_3) δ : 11.77 (brs, 1H), 8.05 (brs, 1H), 7.88 (d, $J = 8.4$ Hz, 2H), 7.49 (d, $J = 7.8$ Hz, 2H), 3.70 (s, 4H), 2.62 (s, 3H), 2.41 (s, 3H), 1.30 (s, 9H); ^{13}C NMR (DMSO- d_6) δ : 163.96, 158.55, 152.41, 147.33, 132.81, 131.91, 127.08, 126.47, 125.68, 101.02, 78.47, 42.80, 30.51, 28.57, 18.36, 13.39; HRMS (EI) m/z 379.1829 M^+ , calc. for $\text{C}_{21}\text{H}_{25}\text{N}_5\text{S}$ 379.1831; Anal. Calc. for: $\text{C}_{21}\text{H}_{25}\text{N}_5\text{S}$ (379): C, 66.46; H, 6.64; N, 18.45%; Found: C, 66.47; H, 6.63; N, 18.44%.

5.1.4.10. 4-(4-(5-(1-(2-(4,5-Dihydro-1H-imidazol-2-yl)hydrazono)ethyl)-4-methylthiazol-2-yl)phenyl)-2-methylbut-3-yn-2-amine (24). Yellowish solid (197 mg, 77%): mp = 127-128 °C.

^1H NMR (DMSO- d_6) δ : 7.97 (brs, 1H), 7.94 (brs, 1H), 7.85 (d, $J = 8.1$ Hz, 2H), 7.49 (d, $J = 8.4$ Hz, 2H), 6.30 (brs, 2H), 3.40 (s, 4H), 2.70 (s, 3H), 2.28 (s, 3H), 1.40 (s, 6H); ^{13}C NMR (DMSO- d_6) δ : 168.97, 161.86, 158.55, 148.33, 132.91, 131.17, 127.10, 126.50, 125.58, 101.02, 78.47, 42.90, 42.61, 30.51, 18.63, 16.34; MS (m/z); 380.2 (M^+ , 42%); HRMS (EI) m/z 380.1780 M^+ , calc. for $\text{C}_{20}\text{H}_{24}\text{N}_6\text{S}$ 380.1783; Anal. Calc. for: $\text{C}_{20}\text{H}_{24}\text{N}_6\text{S}$: C, 63.13; H, 6.36; N, 22.09%; Found: C, 63.12; H, 6.35; N, 22.10%.

5.2. Antimicrobial Testing

5.2.1. Determination of Minimum Inhibitory Concentration (MIC) and Minimum Bactericidal Concentration (MBC) Values. *S. aureus* clinical isolates (NRS107, NRS119, NRS123, VRS10, VRS11a, and VRS12) were obtained through the Network of Antimicrobial Resistance in *Staphylococcus aureus* (NARSA) program and BEI Resources. The MICs of the newly synthesized compounds, tested against clinical isolates of *S. aureus*, were determined using the broth microdilution assay in accordance with the Clinical and Laboratory Standards Institute guidelines [19]. Bacteria were cultured in cation-adjusted Mueller Hinton broth (for *S. aureus*) in a 96-well plate. Compounds, using triplicate samples, were added to the plate and serially diluted. Plates were incubated at 37 °C for at least 20 hours; the MIC was categorized as the concentration at which no visible growth of bacteria was observed. The MBC was determined by transferring a small aliquot (5 μL), from wells lacking bacterial growth (in the MIC plates), onto Tryptic soy agar plates. Plates were incubated at 37 °C for at least 18 hours prior to determining the MBC. The MBC was categorized as the lowest concentration where 99.9% of bacterial growth was inhibited.

5.2.3. Time-kill Assay of Compounds Against MRSA. MRSA cells in logarithmic growth phase ($\text{OD}_{600} > 0.800$) were diluted to $\sim 10^6$ colony-forming units (CFU/mL) and exposed to

concentrations equivalent to $4 \times \text{MIC}$ (in triplicate) of tested compounds (**6**, **10**, and **11** against MRSA UAS300 or **5**, **7**, and **9** against MRSA USA400) and vancomycin in Tryptic soy broth. Aliquots (100 μL) were collected from each treatment after 0, 2, 4, 6, 8, 10, 12, and 24 hours of incubation at 37 °C and subsequently serially diluted in PBS. Bacteria were then transferred to Tryptic soy agar plates and incubated at 37 °C for 18-20 hours before viable CFU/mL was determined.

5.2.4. Cytotoxicity of Compounds Against HRT-18 cells. Compounds exhibiting anti-MRSA activity were assayed (at concentrations of 16, 32, and 64 $\mu\text{g/mL}$) against a human colorectal (HRT-18) cell line to determine the potential toxic effect to mammalian cells *in vitro*. Cells were cultured in RPMI-1640 medium supplemented with 10% fetal horse serum at 37 °C with CO_2 (5%). Control cells received DMSO alone at a concentration equal to that in drug-treated cell samples. The cells were incubated with the compounds (in triplicate) in a 96-well plate at 37 °C with CO_2 (5%) for two hours. The assay reagent MTS 3-(4,5-dimethylthiazol-2-yl)-5-(3-carboxymethoxyphenyl)-2-(4-sulfophenyl)-2H-tetrazolium) (Promega, Madison, WI, USA) was subsequently added and the plate was incubated for four hours. Absorbance readings (at OD_{490}) were taken using a kinetic microplate reader (Molecular Devices, Sunnyvale, CA, USA). The quantity of viable cells after treatment with each compound was expressed as a percentage of the viability of DMSO-treated control cells (average of triplicate wells \pm standard deviation). The toxicity data was analyzed via a one-way ANOVA, with post hoc Dunnet's multiple comparisons test ($P < 0.05$), utilizing GraphPad Prism 6.0 (GraphPad Software, La Jolla, CA).

5.2.5. *In vivo* Pharmacokinetics. Pharmacokinetic studies were performed in male naïve Sprague–Dawley (SD) rats (three animals) following Institutional Animal Care and Use Committee guidelines. An IV bolus of a 2 μM solution was directly administered. Blood samples

were collected over a 12-hour period post dose into Vacutainer tubes containing EDTA-K2. Plasma was isolated, and the concentration of tested compounds in plasma was determined with LC/MS/MS after protein precipitation with acetonitrile. Two-compartmental pharmacokinetic analysis was performed on plasma concentration data in order to calculate pharmacokinetic parameters (Supporting information).

5.2.6. Intracellular Infection of J774 Cells with MRSA and Treatment with Alkynylphenylthiazoles. Compounds **6**, **7**, **9**, **10**, and **11** (8, 16, and 32 $\mu\text{g/mL}$) were assayed against a murine macrophage (J774) cell line to determine the potential toxic effect of the compounds *in vitro*, as described elsewhere [27]. Briefly, cells were cultured in Dulbecco's Modified Eagle Medium (DMEM) supplemented with 10% fetal bovine serum (FBS) at 37 °C with CO₂ (5%). Control cells received DMSO alone at a concentration equal to that in drug-treated cell samples. The cells were incubated with the compounds (in triplicate) in a 96-well plate at 37 °C with CO₂ (5%) for 24 hours. The assay reagent MTS 3-(4,5-dimethylthiazol-2-yl)-5-(3-carboxymethoxyphenyl)-2-(4-sulfophenyl)-2H-tetrazolium) (Promega, Madison, WI, USA) was subsequently added and the plate was incubated for four hours. Absorbance readings (at OD₄₉₀) were taken using a kinetic microplate reader (Molecular Devices, Sunnyvale, CA, USA). The quantity of viable cells after treatment with each compound was expressed as a percentage of the viability of DMSO-treated control cells (average of triplicate wells \pm standard deviation). The toxicity data was analyzed using a Student t-test with post-hoc Holm-Sidak test, ($P < 0.05$), utilizing GraphPad Prism 6.0 (GraphPad Software, La Jolla, CA).

Murine macrophage cells (J774) were cultured in DMEM supplemented with 10% FBS at 37 °C with CO₂ (5%). J774 cells were exposed to MRSA USA400 cells at a multiplicity of infection of approximately 100:1. One-hour post-infection, J774 cells were washed with gentamicin (50

$\mu\text{g/mL}$) to kill extracellular MRSA. Compounds **6** ($16 \mu\text{g/mL}$), **7** ($8 \mu\text{g/mL}$), **9** ($8 \mu\text{g/mL}$), **10** ($16 \mu\text{g/mL}$) and **11** ($16 \mu\text{g/mL}$), and vancomycin (at a concentration equal to $4 \mu\text{g/mL}$) were added to three independent wells. After 24 hours' incubation of compound with infected J774 cells, the test agents were removed; J774 cells were washed with gentamicin ($50 \mu\text{g/mL}$) and subsequently lysed using 0.1% Triton-X 100. The solution was serially diluted in phosphate-buffered saline and transferred to Tryptic soy agar plates in order to determine viable MRSA inside the J774 cells. Plates were incubated at $37 \text{ }^\circ\text{C}$ for 18-22 hours before counting viable CFU/mL. Data are presented as \log_{10} (MRSA CFU/mL) in infected J774 cells.

5.2.7. Examining Alkynylphenylthiazole Ability to Re-sensitize VRSA to Vancomycin.

Compounds **5**, **7**, and **9** were evaluated for their ability to re-sensitize VRSA to the effect of vancomycin using a procedure described in previous studies [5b-d, 6]. Aliquots (5 mL) of the bacterial suspension were divided into microcentrifuge tubes and one compound (at $\frac{1}{2} \times \text{MIC}$) was introduced into each tube. After 30 minutes at room temperature, an aliquot (1 mL) from each tube was transferred to a new centrifuge tube prior to addition of a sub-inhibitory concentration of vancomycin (at a concentration equivalent to $128 \mu\text{g/mL}$). Using a 96-well microtiter plate, rows 2-12 were filled with the remaining bacterial suspension (containing the compound). 200- μL aliquots from tubes containing both the compound and vancomycin were transferred to row 1 of the 96-well plate. Two-fold serial dilutions (in Tryptic soy broth) was completed to dilute the concentration of vancomycin. Untreated bacteria served as a control. Plates were incubated at $37 \text{ }^\circ\text{C}$ for 20-22 hours before the MIC was recorded, as noted above. A fold reduction was calculated by comparing the MIC of vancomycin alone compared to the MIC of the antibiotic given in combination with the compound (at $\frac{1}{2} \times \text{MIC}$).

5.2.8. Evaluation of Alkynylphenylthiazoles and Vancomycin to Reduce the Burden of MRSA USA300 in a *Caenorhabditis elegans* Animal Model. To further investigate the efficacy of the alkynylphenylthiazoles against a MRSA infection, the whole animal model *Caenorhabditis elegans* (*C. elegans*) was utilized. A previously described method was followed with the following modifications [27].

To evaluate the antibacterial activity of the compounds against MRSA *in vivo*, adult worms were transferred to TSA plates seeded with a lawn of MRSA USA300 (highly pathogenic to *C. elegans*) for infection. After six hours of infection, worms were collected and washed with M9 buffer three times before transferring 25-30 worms to wells in a 96-well microtiter plate. Worms were incubated with 20 µg/mL of tested compound (**9** or **11**), vancomycin (positive control), or PBS (negative control) (in triplicate). After treatment for 18 hours, worms were washed three times with M9 buffer and then examined microscopically to examine morphological changes and viability. Worms were subsequently lysed, homogenate serially diluted, and plated onto TSA plates containing 5 µg/mL nalidixic acid to select for MRSA growth. Plates were incubated at 37 °C for 17 hours before viable CFU was determined. MRSA USA300 CFU was divided by the number of worms receiving each treatment and the percent reduction of MRSA in infected worms was subsequently calculated.

5.2.9. UPPS, UPPP Inhibition and IMV Uncoupler Assays. Enzyme inhibition and uncoupler assays were carried out exactly as described previously [6].

5.2.10. MRSA Mice Infection Experiments. Both mice experiments were conducted in accordance with the guidelines of the Purdue University Animal Care and Use Committee (PACUC) and carried out in strict accordance with the recommendations in the Guide for the Care and Use of Laboratory Animals of the National Institutes of Health.

MRSA murine skin infection study: The MRSA mice skin infection study was conducted similar to a previous report [28]. To initiate the formation of a skin wound, five groups (n = 5) of eight-week old female Balb/c mice (obtained from Envigo, Indianapolis, IN, USA) were disinfected with ethanol (70%) and shaved on the middle of the back (approximately a one-inch by one-inch square region around the injection site) one day prior to infection. To prepare the bacterial inoculum, an aliquot of overnight culture of MRSA USA300 was transferred to fresh Tryptic soy broth and shaken at 37 °C until an OD₆₀₀ value of ~1.1 was achieved. The cells were centrifuged, washed once with phosphate-buffered saline (PBS), re-centrifuged, and then re-suspended in PBS. Mice subsequently received an intradermal injection (40 µL) containing 1.32×10^9 CFU/mL MRSA USA300. An open wound formed at the site of injection for each mouse, ~66 hours post-infection. Topical treatment was initiated subsequently with each group of mice receiving the following: fusidic acid (2%, using petroleum jelly as the vehicle), or compounds **9** or **11** (2%, using petroleum jelly as the vehicle). One group of mice was treated with the vehicle alone (negative control). Each group of mice receiving a particular treatment regimen was housed separately in a ventilated cage with appropriate bedding, food, and water. Mice were checked at least four times daily during infection and treatment to ensure no adverse reactions were observed. Mice were treated twice daily for five days, before they were humanely euthanized via CO₂ asphyxiation 12 hours after the last dose was administered. The region around the edge of the skin wound was lightly swabbed with ethanol (70%) and excised. The tissue was subsequently homogenized in PBS (2 mL). The homogenized tissue was then serially diluted in PBS before plating onto mannitol salt agar plates. The plates were incubated for at least 16 hours at 37 °C before viable CFU were counted and MRSA reduction in the skin wound post-treatment was determined for each group.

Neutropenic murine thigh infection study: Female BALB/c mice (obtained from The Jackson Laboratory, Bar Harbor, ME, USA), 6 to 8 weeks old, weighing 19 to 20 grams, were used in this study. All mice were rendered neutropenic via two intraperitoneal (i.p.) injections of 150 and 100 mg/kg of body weight cyclophosphamide four days and one day pre-infection, respectively. To initiate infection, the right thigh of mice was injected with 100 μ L of 5.35×10^7 CFU/mL MRSA USA300. Groups of mice ($n = 5$) were treated twice, two and 12 hours post-infection, with a dose of 20 mg/kg i.p. injection of tested compound (using a vehicle consisting of 10% DMSO, 10% Tween 80, and 80% PBS). Mice receiving a single i.p. injection of the vehicle (10% DMSO, 10% Tween 80, and 80% PBS) two hours post-infection were used as the negative control group. Mice treated twice, two and 12 hours post-infection, with 50 mg/kg vancomycin (prepared in phosphate-buffered saline) administered via i.p. injection served as the positive control group. Three mice were humanely euthanized via CO₂ asphyxiation three hours post-infection in order to determine bacterial load in infected thighs (1.29×10^6 CFU). The remaining groups of mice were humanely euthanized via CO₂ asphyxiation 24 hours post-infection and the right thigh muscle was harvested aseptically. The thighs were weighed and homogenized in PBS using an Omni Tissue Homogenizer (TH115). To determine the bacterial load in the thighs post-treatment, the homogenate was serially diluted in PBS and aliquots (4 μ L) of each dilution were plated on mannitol salt agar plates. The plates were incubated for at least 18 hours at 37 °C before bacterial colonies were enumerated. Data are presented as MRSA CFU/g tissue.

5.3. Permeability Analysis for Compounds 9 and 19. Caco-2 cells were grown in tissue culture flasks, trypsinized, suspended in medium, and were seeded (1×10^5 cells/cm²) onto wells of a Millipore 96-well Caco-2 plate. The cells were allowed to grow and differentiate for three weeks, feeding at two-day intervals. The test compounds were prepared at 10 μ M in HBSS-MES

(pH 6.5) or HBSS-HEPES (pH 7.4) with a final DMSO concentration of 1%. The working solution was then centrifuged and the supernatant was added to the donor side. For Apical to Basolateral (A→B) permeability, the test article was added to the apical (A) side and amount of permeation on the basolateral (B) side was determined; for Basolateral to Apical (B→A) permeability, the test article was added to the B side and the amount of permeation on the A side was determined. To test tight junctions and monolayer integrity, the A-side buffer contained 100 μ M Lucifer yellow dye in Transport Buffer (1.98 g/L glucose in 10 mM HEPES, 1 \times Hank's Balanced Salt Solution) with pH 6.5 while the B-side buffer was Transport Buffer with pH 7.4. Caco-2 cells were incubated with these buffers for 60 minutes (A→B) or 40 minutes (B→A), and the receiver side buffer was removed for analysis by LC/MS/MS. Fluorescein was used as the cell monolayer integrity marker. Fluorescein permeability assessment (A→B direction at pH 7.4 on both sides) was performed after the permeability assay for the test compound. The cell monolayer that had a fluorescein permeability of less than 1.5×10^{-6} cm/s for Caco-2 was considered intact, and the permeability result of the test compound from intact cell monolayer is reported. The apparent permeability coefficient (P_{app}) of the test compound was calculated as follows: $P_{app}(\text{cm/s}) = [(V_R * C_{R,end}) / \Delta t] * [(1 / (A * (C_{D,mid} - C_{R,mid})))]$ where V_R is the volume of the receiver chamber. $C_{R,end}$ is the concentration of the test compound in the receiver chamber at the end time point, Δt is the incubation time and A is the surface area of the cell monolayer. $C_{D,mid}$ is the calculated mid-point concentration of the test compound in the donor side, which is the mean value of the donor concentration at time 0 minute and the donor concentration at the end time point. $C_{R,mid}$ is the mid-point concentration of the test compound in the receiver side, which is one-half of the receiver concentration at the end time point. Concentrations of the test compound were expressed as peak areas of the test compound.

5.4. Metabolic Stability Analysis of Compounds 9 and 19. Each test agent was incubated in duplicate with pooled human liver microsomes at 37 °C. The tested compounds were pre-incubated with pooled human liver microsomes in phosphate buffer (pH 7.4) for five minutes in a 37 °C shaking water bath. The reaction was initiated by adding a NADPH-generating system and incubated for 0, 15, 30, 45, and 60 minutes. The reaction was stopped by transferring the incubation mixture to acetonitrile/methanol. Samples were then mixed and centrifuged. Supernatants were used for HPLC-MS/MS analysis. Data was calculated as percent parent remaining by assuming zero-minute time point peak area ratio (analyte/IS) as 100% and dividing remaining time point peak area ratios by the zero-minute time point peak area ratio. Data were subjected to fit a first-order decay model to calculate both the slope and half-life. Intrinsic clearance was calculated from the half-life and the human liver microsomal protein concentrations using the following equations:

$$CL_{\text{int}} = \ln(2) / (t_{1/2} [\text{microsomal protein}])$$

$$T_{1/2} = 0.693 / -k$$

$$CL_{\text{int}} = \text{intrinsic clearance}; t_{1/2} = \text{half-life}; k = \text{slope}$$

Acknowledgements. This work was funded by the Academy of Scientific Research & Technology (JESOUR-D program, Grant ID# 42) and in part by the United States Public Health Service (NIH grant GM06537). Haroon Mohammad is supported with a fellowship from the Purdue Institute for Drug Discovery. The authors would like to thank BEI Resources, NIAID, and NIH for providing clinical isolates of *S. aureus* used in this study.

References

1. Shanson, D.; Kensit, J.; Duke, R., Outbreak of hospital infection with a strain of *Staphylococcus aureus* resistant to gentamicin and methicillin. *Lancet* **1976**, *308* (7999), 1347-1348.
2. (a) Pantosti, A.; Sanchini, A.; Monaco, M., Mechanisms of antibiotic resistance in *Staphylococcus aureus*. *Future microbiol* **2007**, *2* (3), 323-334; (b) Hope, R.; Livermore, D. M.; Brick, G.; Lillie, M.; Reynolds, R., Non-susceptibility trends among staphylococci from bacteraemias in the UK and Ireland, 2001–06. *J Antimicrob Chemother* **2008**, *62* (suppl 2), ii65-ii74.
3. Chambers, H. F., Treatment of infection and colonization caused by methicillin-resistant *Staphylococcus aureus*. *Infect Control Hosp Epidemiol* **1991**, *12* (01), 29-35.
4. Tommasi, R.; Brown, D. G.; Walkup, G. K.; Manchester, J. I.; Miller, A. A., ESKAPEing the labyrinth of antibacterial discovery. *Nat Rev Drug Discov* **2015**, *14* (8), 529-42.
5. (a) Mohammad, H.; Mayhoub, A. S.; Ghafoor, A.; Soofi, M.; Alajlouni, R. A.; Cushman, M.; Seleem, M. N., Discovery and characterization of potent thiazoles versus methicillin- and vancomycin-resistant *Staphylococcus aureus*. *J Med Chem* **2014**, *57* (4), 1609-15; (b) Mohammad, H.; Reddy, P. V.; Monteleone, D.; Mayhoub, A. S.; Cushman, M.; Hammac, G. K.; Seleem, M. N., Antibacterial Characterization of Novel Synthetic Thiazole Compounds against Methicillin-Resistant *Staphylococcus pseudintermedius*. *PloS one* **2015**, *10* (6), e0130385; (c) Mohammad, H.; Reddy, P. V.; Monteleone, D.; Mayhoub, A. S.; Cushman, M.; Seleem, M. N., Synthesis and antibacterial evaluation of a novel series of synthetic phenylthiazole compounds against methicillin-resistant *Staphylococcus aureus* (MRSA). *Eur J Med Chem* **2015**, *94*, 306-16; (d) Seleem, M. A.; Disouky, A. M.; Mohammad, H.; Abdelghany, T. M.; Mancy, A. S.; Bayoumi, S. A.; Elshafeey, A.; El-Morsy, A.; Seleem, M. N.; Mayhoub, A. S., Second-

Generation Phenylthiazole Antibiotics with Enhanced Pharmacokinetic Properties. *J Med Chem* **2016**, *59* (10), 4900-12.

6. Mohammad, H.; Younis, W.; Chen, L.; Peters, C. E.; Pogliano, J.; Pogliano, K.; Cooper, B.; Zhang, J.; Mayhoub, A.; Oldfield, E.; Cushman, M.; Seleem, M. N., Phenylthiazole Antibacterial Agents Targeting Cell Wall Synthesis Exhibit Potent Activity in Vitro and in Vivo against Vancomycin-Resistant Enterococci. *J. Med. Chem.* **2017**, *60* (6), 2425-2438.

7. Yahia, E.; Mohammad, H.; Abdelghany, T. M.; Fayed, E.; Seleem, M. N.; Mayhoub, A. S., Phenylthiazole antibiotics: A metabolism-guided approach to overcome short duration of action. *Eur J Med Chem* **2017**, *126*, 604-613.

8. Chylek, P.; Robinson, S.; Dubey, M. K.; King, M. D.; Fu, Q.; Clodius, W. B., Comparison of near-infrared and thermal infrared cloud phase detections. *J Geophys Res-Atmos* **2006**, *111* (D20).

9. Crooks, N.; Ross, T.; Grant, S.; Anmolsingh, R.; Gabriel, A.; Foggo-Osseyran, A.; Carroll, K.; Wilson, C., A severe pneumonia due to methicillin resistant *Staphylococcus aureus* clone USA 300: implications of vertical transmission. *West Indian Med. J.* **2012**, *61* (2), 145-7.

10. Desai, P. V.; Sawada, G. A.; Watson, I. A.; Raub, T. J., Integration of in silico and in vitro tools for scaffold optimization during drug discovery: predicting P-glycoprotein efflux. *Mol Pharmaceutics* **2013**, *10* (4), 1249-61.

11. Barry, A. L.; Craig, W. A.; Nadler, H.; Reller, L. B.; Sanders, C. C.; Swenson, J. M., Methods for determining bactericidal activity of antimicrobial agents: approved guideline. *NCCLS Document M26-A* **1999**, *19* (18).

12. Finberg, R. W.; Moellering, R. C.; Tally, F. P.; Craig, W. A.; Pankey, G. A.; Dellinger, E. P.; West, M. A.; Joshi, M.; Linden, P. K.; Rolston, K. V.; Rotschafer, J. C.; Rybak, M. J., The

- importance of bactericidal drugs: future directions in infectious disease. *Clin Infect Dis* **2004**, *39* (9), 1314-20.
13. Nguyen, H. M.; Graber, C. J., Limitations of antibiotic options for invasive infections caused by methicillin-resistant *Staphylococcus aureus*: is combination therapy the answer? *J Antimicrob Chemother* **2010**, *65* (1), 24-36.
14. Krut, O.; Sommer, H.; Kronke, M., Antibiotic-induced persistence of cytotoxic *Staphylococcus aureus* in non-phagocytic cells. *J Antimicrob Chemther* **2004**, *53* (2), 167-73.
15. Cruciani, M.; Gatti, G.; Lazzarini, L.; Furlan, G.; Broccali, G.; Malena, M.; Franchini, C.; Concia, E., Penetration of vancomycin into human lung tissue. *J Antimicrob Chemother* **1996**, *38* (5), 865-869.
16. Moise-Broder, P. A.; Forrest, A.; Birmingham, M. C.; Schentag, J. J., Pharmacodynamics of vancomycin and other antimicrobials in patients with *Staphylococcus aureus* lower respiratory tract infections. *Clin Pharmacokinet* **2004**, *43* (13), 925-942.
17. Pumerantz, A.; Muppidi, K.; Agnihotri, S.; Guerra, C.; Venketaraman, V.; Wang, J.; Betageri, G., Preparation of liposomal vancomycin and intracellular killing of methicillin-resistant *Staphylococcus aureus* (MRSA). *Int J Antimicrob Agents* **2011**, *37* (2), 140-4.
18. (a) Schnedl, W. J.; Mirzaei, S.; Wallner-Liebmann, S. J.; Tafeit, E.; Mangge, H.; Krause, R.; Lipp, R. W., Improvement of Cerebral Hypoperfusion with Levothyroxine Therapy in Hashimoto's Encephalopathy Demonstrated by (99m)Tc-HMPAO-SPECT. *Eur Thyroid J* **2013**, *2* (2), 116-9; (b) Hackl, G.; Milosavljevic, R.; Belaj, K.; Gary, T.; Rief, P.; Hafner, F.; Lipp, R. W.; Brodmann, M., The value of FDG-PET in the diagnosis of thromboangiitis obliterans—a case series. *Clin Rheumatol* **2015**, *34* (4), 739-44.

19. Mohammad, H.; Mayhoub, A. S.; Cushman, M.; Seleem, M. N., Anti-biofilm activity and synergism of novel thiazole compounds with glycopeptide antibiotics against multidrug-resistant staphylococci. *J Antibiot* **2015**, *68* (4), 259-66.
20. Lipp, R. The Innovator Pipeline: Bioavailability Challenges and Advanced Oral Drug Delivery Opportunities <<http://www.americanpharmaceuticalreview.com/Featured-Articles/135982-The-Innovator-Pipeline-Bioavailability-Challenges-and-Advanced-Oral-Drug-Delivery-Opportunities/>> 2013. (accessed May 11, 2017).
21. Hagra, M.; Mohammad, H.; Mandour, M. S.; Hegazy, Y. A.; Ghiaty, A.; Seleem, M. N.; Mayhoub, A. S., Investigating the Antibacterial Activity of Biphenylthiazoles against Methicillin- and Vancomycin-Resistant *Staphylococcus aureus* (MRSA and VRSA). *J Med Chem* **2017**, *60* (9), 4074-4085.
22. Moy, T. I.; Ball, A. R.; Anklesaria, Z.; Casadei, G.; Lewis, K.; Ausubel, F. M., Identification of novel antimicrobials using a live-animal infection model. *Proc Natl Acad Sci U.S.A.* **2006**, *103* (27), 10414-10419.
23. Menzel, R.; Bogaert, T.; Achazi, R., A systematic gene expression screen of *Caenorhabditis elegans* cytochrome P450 genes reveals CYP35 as strongly xenobiotic inducible. *Arch Biochem Biophys* **2001**, *395* (2), 158-68.
24. Hagra, M.; Mohammad, H.; Mandour, M. S.; Hegazy, Y. A.; Ghiaty, A.; Seleem, M. N.; Mayhoub, A. S., Investigating the Antibacterial Activity of Biphenylthiazoles against Methicillin-and Vancomycin-Resistant *Staphylococcus aureus* (MRSA and VRSA). *J Med Chem* **2017**, *60* (9), 4074-4085.
25. (a) Otter, J. A.; French, G. L., Molecular epidemiology of community-associated methicillin-resistant *Staphylococcus aureus* in Europe. *Lancet Infect Dis* **2010**, *10* (4), 227-39; (b)

Nagao, M.; Inuma, Y.; Suzuki, M.; Matsushima, A.; Takakura, S.; Ito, Y.; Ichiyama, S., First outbreak of methicillin-resistant *Staphylococcus aureus* USA300 harboring the Panton-Valentine leukocidin genes among Japanese health care workers and hospitalized patients. *Am J Infect Control* **2010**, *38* (9), e37-e39.

26. (a) Gould, F. K.; Brindle, R.; Chadwick, P. R.; Fraise, A. P.; Hill, S.; Nathwani, D.; Ridgway, G. L.; Spry, M. J.; Warren, R. E., Guidelines (2008) for the prophylaxis and treatment of methicillin-resistant *Staphylococcus aureus* (MRSA) infections in the United Kingdom. *J Antimicrob Chemother* **2009**, *63* (5), 849-61; (b) Moellering, R. C., Jr., Current treatment options for community-acquired methicillin-resistant *Staphylococcus aureus* infection. *Clin Infect Dis* **2008**, *46* (7), 1032-7.

27. Eid, I.; Elsebaei, M. M.; Mohammad, H.; Hagra, M.; Peters, C. E.; Hegazy, Y. A.; Cooper, B.; Pogliano, J.; Pogliano, K.; Abulkhair, H. S.; Seleem, M. N.; Mayhoub, A. S., Arylthiazole antibiotics targeting intracellular methicillin-resistant *Staphylococcus aureus* (MRSA) that interfere with bacterial cell wall synthesis. *Eur J Med Chem* **2017**, *139*, 665-673.

28. Mohammad, H.; Cushman, M.; Seleem, M. N., Antibacterial Evaluation of Synthetic Thiazole Compounds In Vitro and In Vivo in a Methicillin-Resistant *Staphylococcus aureus* (MRSA) Skin Infection Mouse Model. *PloS one* **2015**, *10* (11), e0142321.

Highlights

- Alkynyl-phenylthiazoles can reach intracellular hidden MRSA
- Unlike all other phenylthiazole derivatives, the alkynyl analogues are active systemically
- Phenylthiazoles exerted their antibacterial effect by interfering with bacterial cell wall synthesis
- The most potent analogues inhibited growth of MRSA at concentrations as low as 0.5 $\mu\text{g/mL}$